Peer-reviewed version available at *Int. J. Mol. Sci.* **2020**, *21*, 1995; doi:10.3390/ijms21061995

The aggregation conditions define whether EGCG is an inhibitor or enhancer of α-synuclein amyloid fibril formation

Rebecca Sternke-Hoffmann[1], Alessia Peduzzo[1], Najoua Bolakhrif[1], Rainer Haas[2], and Alexander K. Buell[1,3]

[1]**Institute of Physical Biology, Heinrich-Heine-University Düsseldorf, Germany**
[2]**Department of Hematology, Oncology and Clinical Immunology, Heinrich-Heine-University Düsseldorf**
[3]**Department of Biotechnology and Biomedicine, Technical University of Denmark**

Corresponding author:
Alexander K. Buell[1,2]

Email address: alebu@dtu.dk

ABSTRACT

The amyloid fibril formation by α-synuclein is a hallmark of various neurodegenerative disorders, most notably Parkinson's disease. Epigallocatechin gallate (EGCG) has been reported to be an efficient aggregation inhibitor of numerous proteins, among them α-synuclein. Here we show that this applies only to a small region of relevant parameter space and that under some conditions, EGCG can even accelerate α-synuclein amyloid fibril formation through facilitating its heterogeneous primary nucleation. Furthermore, we show through quantitative seeding experiments that, contrary to previous reports, EGCG is not able to re-model α-synuclein amyloid fibrils into seeding-incompetent structures. Taken together, our results paint a complex picture of EGCG as a compound that can under some conditions inhibit the amyloid fibril formation of α-synuclein, but the inhibitory action is not robust against various physiologically relevant changes in experimental conditions. Our results are important for the development of strategies to identify and characterise promising amyloid inhibitors.

INTRODUCTION

The misfolding and uncontrolled aggregation of proteins is linked to the onset and progression of a range of neurological disorders, such as Parkinson's disease (PD) and Alzheimer's disease (Braak and Braak, 1991; Knowles et al., 2014; Chiti and Dobson, 2017). PD is a progressive disorder of the nervous system that affects movement, but it also has non-motor symptoms. A pathological characteristic of PD are Lewy bodies (Aarsland et al., 2009). The major filamentous component of Lewy bodies is the presynaptic protein α-synuclein (Baba et al., 1998; Spillantini et al., 1998; Luk et al., 2012).

α-synuclein is a 140-residue neuronal protein, which can aggregate into highly ordered, cross-β-sheet structured amyloid fibrils (Guerrero-Ferreira et al., 2018). The aggregation mechanism of α-synuclein is a complex nucleation-dependent polymerization process, which manifests itself in test tube experiments of aggregation kinetics through a lag phase, followed by a growth and a steady state phases (Wood et al., 1999). At a molecular level, this involves different microscopic steps, in particular (heterogeneous) primary nucleation and growth, and, depending on the solution conditions, fragmentation and secondary nucleation (Knowles et al., 2014; Buell et al., 2014).

At neutral pH α-synuclein carries a net negative charge, due to its isoelectric point of 4.0-4.7 (Uversky et al., 2001). The protein adopts a primarily disordered conformation without well defined secondary or tertiary structure (intrinsically disordered conformation) (Bertoncini et al., 2005; Theillet et al., 2016). At low pH, α-synuclein displays a more compact conformation due to a collapse of the normally highly acidic and extended C-terminal tail (McClendon et al., 2009). The C-terminal tail becomes fully protonated, thus uncharged, and it forms a compact conformational ensemble with increased hydrophobicity, resulting in an accelerated α-synuclein fibril formation at low pH (Buell et al., 2014); a similar effect can be achieved

by truncating the C-terminus (van der Wateren et al., 2018). Compared to aggregation at neutral pH, the aggregation process is strongly enhanced at mildly acidic pH values (pH < 6), through an efficient production of new growing fibrils catalysed by the binding to the surfaces of pre-existing fibrils (secondary nucleation) (Buell et al., 2014; Gaspar et al., 2017). The investigation of the behaviour of α-synuclein at mildly acidic pH values is physiologically relevant, because α-synculein can experience such solution conditions during its life cycle in endosomes and lysosomes, which maintain an acidic pH value between 4 and 5 (Pillay et al., 2002; Mak et al., 2010; Bourdenx et al., 2014). This lower pH has to be considered when designing a possible therapeutic strategy for the treatment of neurodegenerative disorders.

Once formed, amyloid aggregates are often highly stable and it is difficult to reverse the aggregation process and to prevent it from spreading through secondary processes. Therefore the development of inhibitors that are able to prevent the initial formation of amyloid aggregates is crucial. In particular, a target of these substances are small oligomeric species, which are suspected to be the most cytotoxic (Bucciantini et al., 2002), has been proposed to be an efficient strategy to combat neurodegenerative diseases. Viable therapeutic strategies for prevention and treatment of amyloid-related diseases are 1) the maintenance of the amyloidogenic protein in its soluble state, 2) the redirection of the amyloidogenic proteins into unstructured, nontoxic and off-pathway aggregates and 3) remodeling and/or dissociation of the mature amyloid fibrils. One class of inhibitors of α-synuclein amyloid fibril formation is formed by molecules that can interact with amyloidogenic monomers in order to prevent their inter-molecular associations, such as antibodies or affibodies (Iljina et al., 2017; Agerschou et al., 2019). Small molecules have also been proposed as inhibitors of α-synuclein amyloid fibril formation (Wagner et al., 2013; Tóth et al., 2014; Perni et al., 2017; na Díaz et al., 2019). These include polyols, polyphenols or other aromatic molecules containing hydrogen-bonding functionalities. Polyphenols are naturally occurring secondary metabolites of plants characterized by the presence of two or more phenol rings (Pandey and Rizvi, 2009). A well-studied polyphenol is Epigallocatechin-3-gallate (EGCG), the main polyphenol found in green tea. Biochemical studies indicate the neuroprotective action of EGCG, which has been suggested to effectively inhibit the aggregation of a number of amyloidogenic peptides and proteins, including α-synuclein (Bieschke et al., 2010; Zhao et al., 2017; Qing et al., 2016; Roy and Bhat, 2019; Teng et al., 2019), amyloid-β (related to AD) (Liu et al., 2015; Bieschke et al., 2010), islet amyloid polypeptide (related to type-II diabetes) (Lee et al., 2019; Xu et al., 2017), huntingtin exon 1 (related to Huntington's disease) (Ehrnhoefer et al., 2006), tau (related to AD and tauopathies) (Wobst et al., 2015), superoxide dismutase (related to amyotrophic lateral sclerosis) (Srinivasan and Rajasekaran, 2017), prion proteins (related to prion diseases) (Rambold et al., 2008; Roberts et al., 2009) and others. EGCG has the ability to prevent the formation of toxic prefibrillar oligomers as well as to inhibit amyloid fibril formation and has been proposed to remodel existing amyloid fibrils. Most of the studies are performed at physiological pH, where EGCG is unstable and auto-oxidises fast into various products (Wei et al., 2016). Decreasing the pH to slight acidic pH values ($\leq$ pH 6), results in a considerable increase in EGCG stability, which we have recently shown to lead to a strongly impaired ability of EGCG to inhibit α-synuclein aggregation (Sneideris et al., 2019). Considering that both α-synuclein and EGCG are likely to encounter such pH environments *in vivo*, the aim of the present study is to characterise in more detail the dependence of EGCG inhibition of α-synuclein aggregation on the solution conditions. The *in vitro* amyloid fibril formation of α-synuclein is an intrinsically slow process, due to the fact that the primary nucleation process is heterogeneous and requires a combination of appropriate surfaces (e.g. air-water interface (Campioni et al., 2014), polymer-water interface (Grey et al., 2011) or lipid-water interface (Galvagnion et al., 2015)) and constant agitation of the sample. The nucleation step can be bypassed by the addition of exogenous fibrils (seeds). Seeding, in particular at high seed concentrations (where all molecular processes other than fibril growth can be neglected (Buell, 2019)) can improve the reproducibility of the aggregation kinetics of α-synuclein. In this study we payed special attention on how the effect of EGCG on the fibril formation is altered, when the aggregation of α-synuclein is studied under different conditions, such as different surfaces and the presence and absence of glass beads. By systematically examining a wide range of pH values, we probe the influence of EGCG oxidation and the interplay between the solution conditions and the action of EGCG. Overall we find that EGCG is an efficient inhibitor of α-synuclein aggregation only in a small range of parameter space. Under some conditions, especially those that lead to enhanced stability of EGCG, it can either have no effect on the amyloid fibril formation of α-synuclein or even promote the latter.

Preprints (www.preprints.org) | NOT PEER-REVIEWED | Posted: 3 February 2020 doi:10.20944/preprints202002.0018.v1

Peer-reviewed version available at Int. J. Mol. Sci. 2020, 21, 1995; doi:10.3390/ijms21061995

MATERIAL AND METHODS

Materials and Solutions

α-synuclein in the pT7-7 vector was expressed in *E. coli* BL21 (DE3) and purified as previously described (Peduzzo et al., 2019; **?**). As a last step α-synuclein was purified by size-exclusion chromatography on an ÄKTA pure chromatography system (GE Healthcare) using a Superdex 200 Increase 10/300 GL (GE Healthcare) and 20 mM citric acid, pH 7, as an elution buffer. α-synuclein concentration was determined by measuring UV-absorption at 275 nm (extinction coefficient of 5600 M^{-1} cm^{-1}). For the α-synuclein inhibition experiments, 5 mM solutions of EGCG (Tocris #4524) were prepared by dissolving EGCG in dH_2O. The EGCG solutions were frozen and stored at -20°C, after monitoring no difference between freshly dissolved and thawed EGCG. $EGCG_{ox}$ was prepared by dissolving 10 mM of EGCG in 20 mM citric acid, pH 7, and incubating for at least 6 hours at 60°C in a thermomixer compact (Eppendorf) at 1000 rpm. Subsequently, it was diluted to a final concentration of 5 mM, frozen and stored at -20°C.

Measurements of Aggregation Kinetics

In order to study the effect of EGCG of the amyloid fibril formation by α-synuclein, solutions of 25 μM of α-synuclein were prepared with EGCG or $EGCG_{ox}$ solutions in a 1:1 and 1:5 (protein:compound) ratio, 20 μM ThT and 150 mM citric acid at the desired pH value (pH 3, pH 4, pH 5, pH 6 or pH 7). 3 replicates of each solution were then pipetted into a high-binding surface plate (Corning #3601) or a non-binding surface plate (Corning #3881). The aggregation kinetics were monitored in the presence and absence of small glass beads (SiLibeads Typ M, 3.0 mm). The plates were sealed using SealPlate film (Sigma-Aldrich #Z369667). The kinetics of amyloid fibril formation were monitored at 37°C under continuous shaking (300 rpm) or quiescent conditions by measuring ThT fluorescence intensity through the bottom of the plate using a FLUOstar (BMG LABTECH, Germany) microplate reader (readings were taken every 5 min).

In order to investigate the interactions of EGCG and the surface of the non-binding surface plate, 130 μL of solutions of EGCG or $EGCG_{ox}$ (25 μM and 125 μM) were pipetted into a well and incubated at room temperature for 2 h. After incubation, the solutions were removed, the concentration of EGCG and $EGCG_{ox}$ were measured by UV-absorption and a solution of 25 μM α-synuclein, 20 μM ThT and 150 mM citric acid pH 4 was added to the pre-treated wells. 3 replicates per condition were measured. The $EGCG_{ox}$ concentration was compared to a solution which was incubated in an Eppendorf tube. The highest ThT fluorescence emission value within each time course was taken to be I_{max}. The half-times (t_{50}) of the aggregation reaction were obtained as described by Meisl *et al.* (Meisl et al., 2016).

Seeded Aggregation Experiments

In order to probe the effects of EGCG and $EGCG_{ox}$ particularly on the elongation process and on preformed fibrils, the aggregation kinetics of α-synuclein were monitored in the presence of 5 % and 0.5 % seeds in relation to the used monomer concentration. For the preparation of the seeds, solutions of 50 μM α-synuclein were incubated at 37°C in a high-binding surface plate, in the presence of glass beads and under continuous shaking at the desired pH-values (pH 3, pH 4, pH 5, pH 6 or pH 7). The end product after 24 h of incubation, when the reaction was found to be completed under all conditions, was used to seed fresh solutions of 50 μM α-synuclein, which were incubated at 37°C for 24 h in an Eppendorf Thermomixer with continuous shaking (1200 rpm). The product of this seeded aggregation experiment was used to seed the kinetic experiments in the presence and absence of EGCG and $EGCG_{ox}$. For the calculation of the seed concentration, it was assumed that the monomer had quantitatively converted to amyloid fibrils. Before performing the experiment, the seed-solutions were homogenized using an ultra-sonication bath Sonorex RK 100 H (Bandelin, Germany) for 180 s. The seeded aggregation experiments were performed in non-binding surface plates with 25 μM α-synuclein monomer and the preformed fibrils were added as seeds to a final concentration of 0.5 or 5 % of the monomer solution at the desired pH value. For the experiment with seeds that were to be pre-incubated with EGCG, we added 50 μM EGCG or $EGCG_{ox}$ to a solution of 50 μM α-synuclein fibrils, at pH 5, pH 6 and pH 7. After 2 h the fibrils were added to 25 μM monomer at the corresponding pH value to a final concentration of 5% and the aggregation kinetics were recorded every 150 s. In order to investigate if EGCG can remodel pre-formed fibrils, we incubated 10 μM fibril solutions, which were sonicated beforehand, with 10 μM EGCG or $EGCG_{ox}$ in a non-binding surface plate at 37°C under shaking conditions at pH 6 or pH 7 for over 100 h. The fluorescence intensity was recorded using a FLUOstar (BMG LABTECH) microplate reader

(readouts were taken every 5 min). After the incubation 50 μM fresh monomer was added to the solutions and the measurement was continued, with readings taken every 150 s, allowing a potential change in the seeding efficiency to be detected.

Atomic Force Microscopy (AFM)

AFM images were acquired directly after the aggregation kinetic measurements. 10 μL of each sample was deposited onto freshly cleaved mica. After drying, the samples were washed 5 times with 100 μL of dH_2O and dried under gentle flow of nitrogen. AFM images were obtained using a NanoScope V (Bruker) atomic force microscope equipped with a silicon cantilever ScanAsyst-Air with a tip radius of 2-12 nm.

Microfluidic diffusional sizing and concentration measurements

Fluidity One is a microfluidic diffusional sizing (MDS, (Arosio et al., 2015)) device, which measures the rate of diffusion of protein species under steady state laminar flow and determines the average particle size from the overall diffusion coefficient. The protein concentration is determined by fluorescence intensity, as the protein is mixed with ortho-phthalaldehyde (OPA) after the diffusion, a compound which reacts with primary amines, producing a fluorescent compound (Yates et al., 2015). To measure the concentration of the soluble α-synuclein, the samples were centrifuged for 60 min at 16100 g at 25°C using centrifuge 5415 R (Eppendorf) directly after the kinetic measurements. The top half of the supernatant was removed and 6 μL of this solution was pipetted onto a disposable microfluidic chip and measured with the Fluidity One (F1, Fluidic Analytics, Cambridge, UK). For the measurement of the amount of protein in the pellet, the pellet was re-suspended in the remaining liquid and 6 μL of this solution was pipetted onto a microfluidic chip and analysed with the F1 instrument.

RESULTS

Non-seeded experiments in high-binding plates

We performed α-synuclein amyloid fibril formation experiments in high-binding surface plates in the presence and absence of glass beads under shaking conditions (Figure 1). α-synuclein monomer solutions are kinetically highly stable, because the homogeneous primary nucleation rate is slow, in particular around neutral pH. Under most conditions, the primary nucleation of α-synuclein is triggered by surfaces that have an affinity for the protein. When α-synuclein binds to a suitable surface or interface, the N-terminal domain can adopt a helical structure (Fusco et al., 2014), which seems to facilitate the formation of fibril nuclei and oligomers. The air-water-interface (Campioni et al., 2014), the surface of the plate (Grey et al., 2011) and, under mildly acidic pH conditions, the surface of already formed fibrils (Buell et al., 2014; Gaspar et al., 2017) function as a nucleation assistance. The growing fibrils can then be fragmented by the shaking, in particular in the presence of glass beads (Buell et al., 2014), which leads to accelerated aggregation kinetics. We therefore performed aggregation experiments either in the presence or absence of glass beads.

α-synuclein monomers were combined with the compound EGCG or $EGCG_{ox}$ in a protein:compound ratio of 1:1 (25μM:25μM) or 1:5 (25μM:125μM) and the aggregation was monitored through the change in Thioflavin-T (ThT) fluorescence intensity. An increase in the intensity indicates the formation of ThT-positive aggregates specifically amyloid fibrils. The results of these initial experiments in polystyrene plates are shown in Figure 1, and the extracted maximal fluorescence intensities and aggregation half times are shown in Figure 2. The half time (t_{50}) is the time point when the ThT intensity has reached half the value between the initial baseline and the final plateau value and can be used as a macroscopic parameter to describe the aggregation kinetics. α-synuclein displayed the fastest aggregation kinetics at pH 4 with a t_{50} of 1.1 h when glass beads were added. Without glass beads the fibril formation was slowed down by a factor of 2. The *de novo* aggregation at pH 3 and pH 5 is similar, and the kinetics under these two conditions are slower by a factor of 2-3 (with added glass beads) and 8 (without additional glass beads), compared to pH 4. The aggregation at pH 5 is slightly faster than at pH 3 and the influence of the glass beads on the kinetics is bigger. The glass beads have the strongest aggregation enhancing influence at pH 7. α-synuclein can not form amyloid fibrils very efficiently at pH 7, possibly due to the high negative charge under these conditions, which is not strongly screened at the moderate ionic strength values of our experiments. Since the secondary nucleation is suppressed at neutral pH, the dominating aggregation events are only primary nucleation and elongation of the newly formed fibrils. In the presence

Preprints (www.preprints.org) | NOT PEER-REVIEWED | Posted: 3 February 2020 doi:10.20944/preprints202002.0018.v1

Peer-reviewed version available at Int. J. Mol. Sci. 2020, 21, 1995; doi:10.3390/ijms21061995

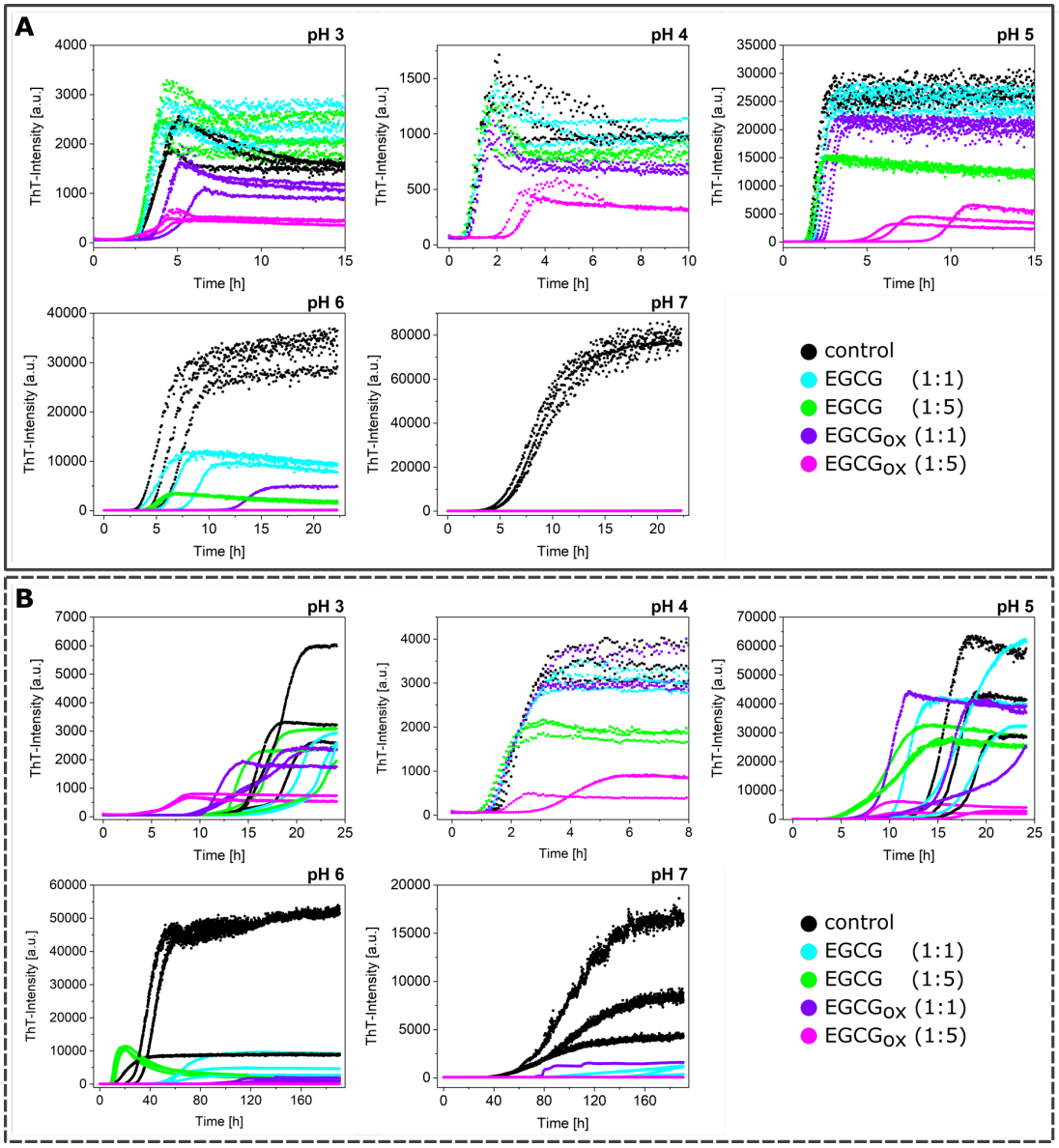

Figure 1. The effects of different ratios (1:1 and 5:1 with respect to protein) of EGCG and EGCG$_{ox}$ on the aggregation kinetics of α-synuclein at different pH values (pH 3 to pH 7), monitored in high-binding surface plates in the presence (A) and absence (B) of glass beads. A small subset of this data (pH 6 and pH 7, 1:1 EGCG and 1:1 EGCG$_{ox}$) is from (Sneideris et al., 2019).

of glass beads the enhanced fragmentation leads to a t_{50} of 9 h, whereby the absence of glass beads leads to an almost complete absence of secondary processes and a t_{50} of 96 h.

Due to the spectroscopic features of the ThT to increase its fluorescence intensity upon binding to amyloid fibrils, it is possible to consider the enhanced ThT fluorescence intensity as an increase in the concentration of aggregates that are formed. When the maximal ThT fluorescence intensities are compared to I_{max} of the control, i.e. the absence of either EGCG or EGCG$_{ox}$, almost all conditions show a decrease, in particular at neutral and slightly acidic pH (pH 7 - pH 6) (Figure 2). Only the aggregation at pH 3 shows an increased fluorescence intensity in the presence of EGCG. In the presence of EGCG$_{ox}$ the intensities are decreased under all conditions indicating either an inhibitory effect on the aggregation or an interference with the ThT-signal. When the experiments were performed without glass beads, I_{max} showed a similar outcome. However, at pH 3 the intensities are decreased in the presence of EGCG and EGCG$_{ox}$ when the glass beads were removed.

Preprints (www.preprints.org) | NOT PEER-REVIEWED | Posted: 3 February 2020 doi:10.20944/preprints202002.0018.v1

Peer-reviewed version available at Int. J. Mol. Sci. 2020, 21, 1995; doi:10.3390/ijms21061995

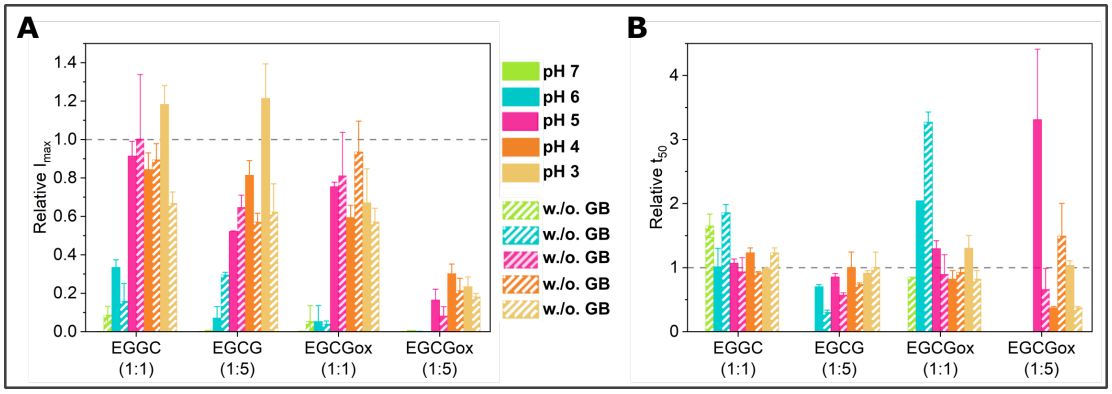

Figure 2. Overview of the effects of EGCG and $EGCG_{ox}$ on α-synuclein aggregation monitored in a high-binding surface plates assayed by (A) maximum ThT fluorescence intensity and (B) t_{50} of the aggregation time course. Filled bars represent aggregation in the presence of glass beads, striped bars in the absence of glass beads. Error bars are standard deviations. The data is normalized to the control of the corresponding condition, i.e. the aggregation in the absence of EGCG or $EGCG_{ox}$, the kinetic parameters of which are indicated with the horizontal dashed line at a factor of 1. Relative t_{50} values are only displayed, if any fibril formation is detected by an increase in ThT fluorescence intensity.

If rather than I_{max}, the half-time of the aggregation reaction, t_{50}, is used as a read out, the observed inhibitory effects of EGCG at neutral and slightly acidic pH (pH 7 and pH 6) are different. At pH 7 and in the presence of EGCG there is no increase in ThT-signal observable in the presence of glass beads, whereas there is a slight increase in fluorescence intensity over time in the absence of glass beads. In one of the three repeats in the presence of $EGCG_{ox}$, a minor fluorescence intensity increase has been also observed in the case of the equimolar ratio EGCG to protein. The t_{50} of the aggregation in the presence of EGCG is clearly increased at pH 7. The picture at pH 6, however, is different. Where in the presence of EGCG (1:1) the intensity was significantly ($p \leq 0.01$) decreased, the t_{50} is not distinguishable from the control. In the presence of a high concentration of EGCG, the kinetics are faster both with and without additional glass beads. However the ThT-intensity curves without glass beads did not show the typical sigmoidal shape. The decrease of the signal at longer times could be explained by higher order assembly or surface adsorption of the amyloid fibrils (Murray et al., 2013), or else a time dependent interference of EGCG with ThT fluorescence. In the presence of $EGCG_{ox}$ the kinetics are prolonged and even completely inhibited, both with and without glass beads. However, quantification of the soluble protein in the supernatant at the end of the experiment with additional glass beads showed a loss of 62-67% in the presence of $EGCG_{ox}$ (1:1) and (1:5). The formed aggregates are accordingly either not ThT-positive or else the EGCG interferes too strongly with their ThT fluorescence.

At more acidic pH values, only the oxidised form of the EGCG showed any clear effect on the aggregation kinetics. At pH 5 and pH 4 the $EGCG_{ox}$ (1:5) showed a significant increase of t_{50}, but in the absence of glass beads the EGCG showed an accelerating effect at pH 5 and pH 3. At pH 4 the aggregation kinetics are slowed down slightly, but not as much as in the presence of glass beads and it is not statistically significant. The variability in the kinetics of the three replicates per condition, especially at pH 3 and pH 5, is high, rendering a thorough statistical analysis difficult with such a small number of replicates.

Non-seeded experiments in non-binding plates

The amyloid formation of α-synuclein is favoured in high-binding surface plates, due to the ability of the polystyrene-water interface to provide nucleation sites. In an attempt to try and disentangle the effects of EGCG and $EGCG_{ox}$ on the polystyrene surface-induced nucleation from that on other relevant processes, we also performed aggregation experiments in non-binding surface plates, i.e. plates where the surface is coated with a protein-repellent PEG layer (Figure 3). These non-binding surface plates are often used in kinetic experiments of amyloid fibril formation in order to minimize the contribution of heterogeneous nucleation processes and therefore simplify the kinetic analysis (Cohen et al., 2013; Buell et al., 2014; Galvagnion et al., 2015). As expected, therefore, the kinetics of *de novo* aggregation in the non-binding

Preprints (www.preprints.org) | NOT PEER-REVIEWED | Posted: 3 February 2020 doi:10.20944/preprints202002.0018.v1

Peer-reviewed version available at Int. J. Mol. Sci. 2020, 21, 1995; doi:10.3390/ijms21061995

surface plates are slowed down with respect to the high-binding plates, but the high fragmentation rate in the presence of glass beads allows fibril formation to be observed within an experimentally accessible time scale. The enhanced fragmentation amplifies the fibrils that form at the air-water interface (Campioni et al., 2014). This difference in lag times between high and low binding plates is particularly pronounced at the pH values which lead to very fast aggregation kinetics in the high-binding surface plates: at pH 4 the t_{50} is increased by a factor of 3.4, whereas it is only increased by a factor of 1.3 at pH 7.

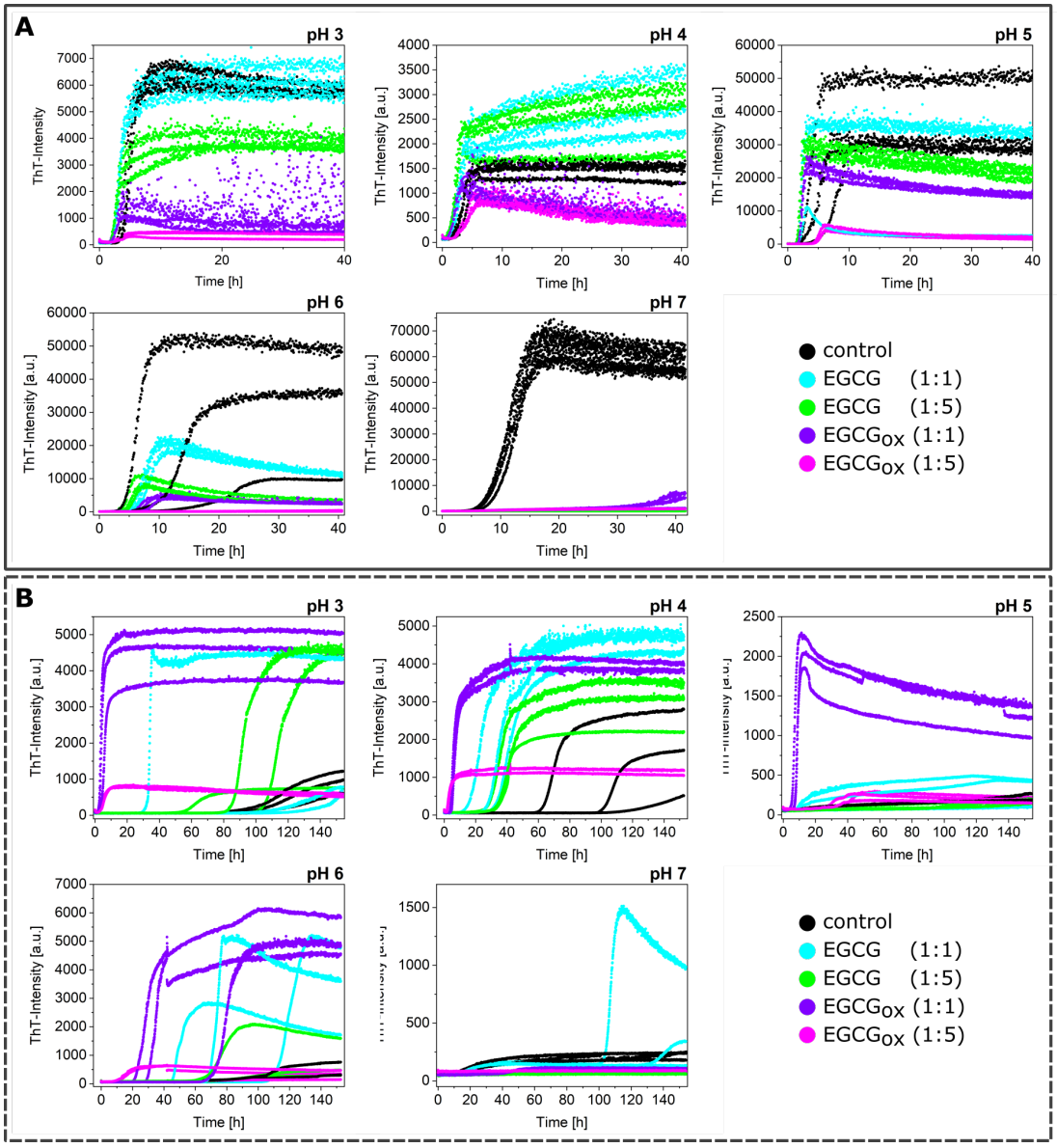

Figure 3. The effects of EGCG and $EGCG_{ox}$ on the aggregation kinetics of α-synuclein at different pH values (pH 3 to pH 7) monitored in a non-binding surface plate in the presence (A) and absence (B) of glass beads.

While the maximal ThT-intensities in the presence of glass beads and EGCG or $EGCG_{ox}$ in non-binding plates are comparable to the aggregation experiments conducted in a high-binding surface plate, the t_{50}s indicated an aggregation-enhancing effect of both oxidized and fresh EGCG (Figure 4).

The enhanced fragmentation of the fibrils by the use of glass beads leads in general to more reproducible data, both in binding and non-binding plates. However, the aggregation kinetics under some conditions (e.g. pH 6) is still rather variable, as both I_{max} and t_{50} differ between the three replicates of the control sample. In order to obtain an independent (of ThT fluorescence intensity) measurement

Preprints (www.preprints.org) | NOT PEER-REVIEWED | Posted: 3 February 2020 doi:10.20944/preprints202002.0018.v1

Peer-reviewed version available at Int. J. Mol. Sci. 2020, 21, 1995; doi:10.3390/ijms21061995

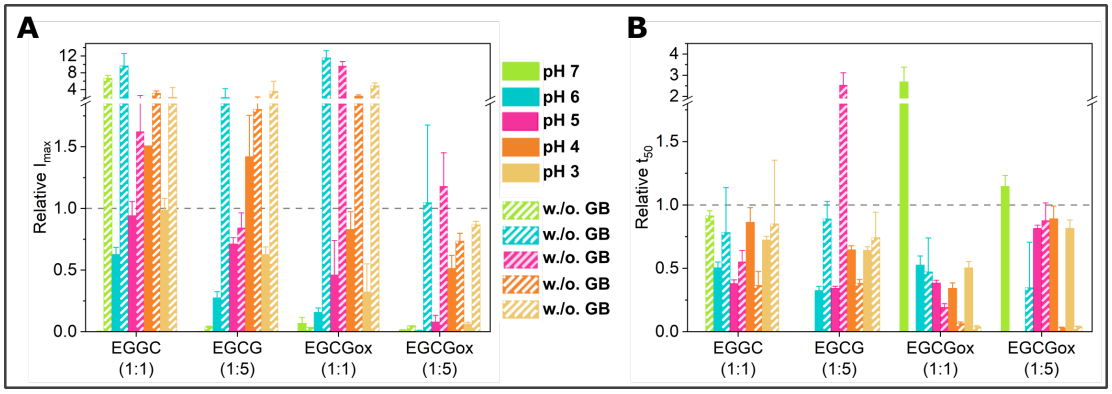

Figure 4. Overview of the effects of EGCG and $EGCG_{ox}$ on α-synuclein aggregation monitored in a non-binding surface plate assayed by (A) maximum ThT fluorescence intensity and (B) t_{50} of the aggregation. Filled bars represent aggregation in presence of glass beads, striped bars without glass beads. Error bars are standard deviations. The data is normalized to the control of the corresponding condition, the comparison is outlined with the dashed line (at 1).

of aggregate mass in this case, we centrifuged the samples at the end point of the experiments and measured the size and concentration of the soluble α-synuclein in the supernatant (Figure 5 A, left panel) by microfluidic diffusional sizing (MDS) (Arosio et al., 2015). We found that while the ThT-signal displayed a clear difference, the amount of soluble protein in the supernatant is similar. In all three samples α-synuclein converts near-quantitatively into aggregates, and the average size of the supernatant fraction is that of monomeric protein. Overall, the picture that emerges from these ThT experiments in non-binding plates with added glass beads is that EGCG and $EGCG_{ox}$ only have an inhibitory effect at pH 7 and in addition at pH 6 in the presence of a 5-fold excess of $EGCG_{ox}$. This conclusion is confirmed by MDS experiments under all conditions (Figure 5 A, central panel), which show that despite the variable final ThT intensity, the protein is quantitatively converted into fibrils, illustrating that EGCG and $EGCG_{ox}$ can have a strong influence on ThT intensity (Sneideris et al., 2019).

In the absence of glass beads, the aggregation curves are generally more variable also in the non-binding surface plate. The absolute fluorescence intensities at the plateau were increased by a factor of up to almost 10 in the presence of EGCG (for example at pH 6 with EGCG and $EGCG_{ox}$ (1:1) and pH 5 with $EGCG_{ox}$ (1:1)), and only in the presence of the 5-fold excess of oxidised EGCG we could detect similar or slightly decreased maximal intensities compared to the control. Importantly, the aggregation kinetics in the absence of glass beads are accelerated with respect to the control in the presence of both oxidised and fresh EGCG, in particular by the former. This accelerating effect is particularly pronounced at acidic pH (pH 3 and 4), but also observed at pH 5 and 6. Again, only at pH 7, an inhibitory effect is observed. The control aggregation (no EGCG) at pH 7 in the absence of glass beads displayed a peculiar characteristic: the ThT fluorescence increase starts already after ca. 10 h, but the rate of increase in fluorescence intensity was slow. The analysis of the supernatant after more than 100 h demonstrated that over 80% of the protein was still soluble and had an average radius of 3.12 nm (Figure 5 B), corresponding to the expected size of the monomer (Gang et al., 2018). The lag time of the sample with an equimolar concentration of EGCG was slightly longer, but the reaction reached a much higher final fluorescence level. All the other samples at pH 7 without glass beads did not show any fluorescence intensity increase. We also probed for the presence of fibrils and the degree of aggregation under those conditions with the help of AFM-imaging and MDS. In these MDS experiments, we measured both the pellet and the supernatant and calculated the total concentration that the MDS data could account for. Based on the observation that the combined concentrations in both pellet and supernatant did not add up to the initially used concentration, we concluded that the samples with 1:5 EGCG and those 1:1 and 1:5 EGCG $_{ox}$ also aggregated, but the aggregates were not ThT-positive (either due to their non-fibrillar nature or due to quenching by EGCG) and were probably too big to be quantifiable by MDS. This is compatible with the observation that in all samples, except for the one with 1:1 EGCG, the α-synuclein was still primarily monomeric with radii between 2.4 and 3 nm.

At pH 4, in non-binding plates and in the absence of glass beads, all EGCG and $EGCG_{ox}$ containing

Preprints (www.preprints.org) | NOT PEER-REVIEWED | Posted: 3 February 2020 doi:10.20944/preprints202002.0018.v1

Peer-reviewed version available at Int. J. Mol. Sci. 2020, 21, 1995; doi:10.3390/ijms21061995

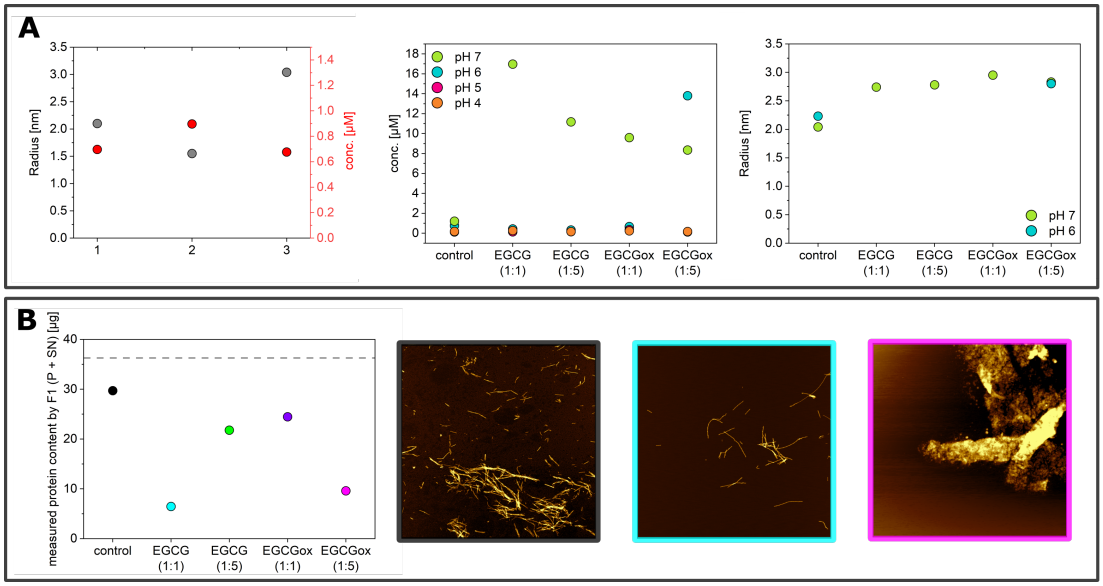

Figure 5. (A) Soluble α-synuclein concentration measured in the supernatant after centrifuging the end product of the aggregation reactions in a non-binding surface plate in the presence of glass beads. Radius in nm and concentration in μM of the three replicates of α-synuclein at pH 6 (control) (left), concentration in μM (middle) and radius in nm (right) of the end product of the aggregation reactions at pH 4, pH 5, pH 6 and pH 7. The three replicates per condition were combined before centrifugation (except for the control at pH 6, where each replicate sample was analysed separately, see A). (B) Amount of protein measurable with the Fluidity One (F1) MDS instrument (supernatant + pellet) in μg in the end-product of α-synuclein at pH 7 in a non-binding surface plate without additional glass beads (left). The dotted line indicates the used amount of protein. AFM-height-images of the control (black frame), α-synuclein with EGCG (1:1) (cyan frame) and of α-synuclein with EGCG$_{ox}$ (1:5) (magenta frame). The image scale is 5 x 5 μM. The colour range represents the height from -2 to 10 nm (left and middle) and -10 to 25 nm (right).

samples showed faster and more reproducible aggregation than the control samples. In order to probe whether the type of aggregates formed under all these conditions is the same, we performed time-resolved AFM imaging experiments. Aliquots were taken at different time points directly out of the plate during the measurement (Figure 3B) and imaged by AFM (Figure 6). The sample of α-synuclein with a 5-fold excess of EGCG$_{ox}$ (1:5) (magenta frame) displayed many short fibrils and some amorphous structures after 17 h, when the ThT-signal had already reached the plateau-phase for several hours. For the other samples, we only found fibrils under all conditions in the last time point. At 17 h and 42 h, for example, we could not find any aggregates in the control and 1:1 EGCG$_{ox}$ samples, even if the ThT-signal displayed fibril formation, highlighting the fact that imaging-based analysis alone can be unreliable in some cases. Overall, we found no clear difference in appearance of the fibrils made under any of the different EGCG regimes at pH 4, confirming that neither EGCG nor EGCG$_{ox}$ displays an inhibiting effect under these conditions, and that the observed accelerated emergence of ThT fluorecence can indeed be ascribed to an enhancing effect of the EGCG.

As described above, α-synuclein normally requires an appropriate surface or interface, to induce the nucleation of its amyloid fibrils. Therefore the question arises as to how EGCG is able to accelerate the formation of amyloid fibrils in non-binding surface plates. It could be that EGCG directly interacts with the monomeric α-synuclein and facilitates nucleation or else, the EGCG interacts with the non-binding plate surface and renders it conducive to induce α-synuclein amyloid fibril nucleation. We hypothesised that if EGCG has a high affinity for the non-binding plate surface, pre-treatment of the plate with EGCG should have a comparable effect as if the ECGG was present during the entire aggregation experiment. Therefore, we incubated wells for two hours at room temperature with solutions of 25 μM (corresponding to 1:1 EGCG) or 125 μM EGCG or EGCG$_{ox}$ (corresponding to 1:5 EGCG). After incubation the solution was removed and the concentration of EGCG in the removed solution was determined. We found that the

Preprints (www.preprints.org) | NOT PEER-REVIEWED | Posted: 3 February 2020 doi:10.20944/preprints202002.0018.v1

Peer-reviewed version available at Int. J. Mol. Sci. 2020, 21, 1995; doi:10.3390/ijms21061995

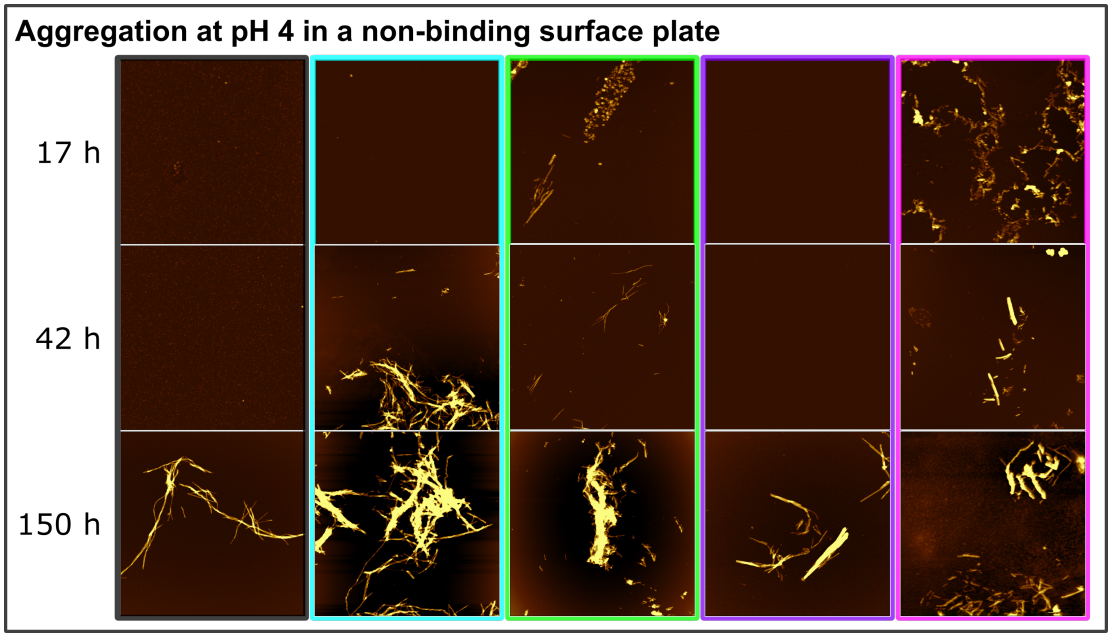

Figure 6. Time-resolved AFM-height-images of α-synuclein aggregation at pH 4 in a non-binding surface plate without glass beads. The colors of the frame correspond to the condition (Figure 3): control (black frame), EGCG (1:1) (cyan frame), EGCG (1:5) (green frame), $EGCG_{ox}$ (1:1) (purple frame) and $EGCG_{ox}$ (1:5) (magenta frame). The image scale is 5 x 5 μM. The colour range represents the height from -5 to 20 nm.

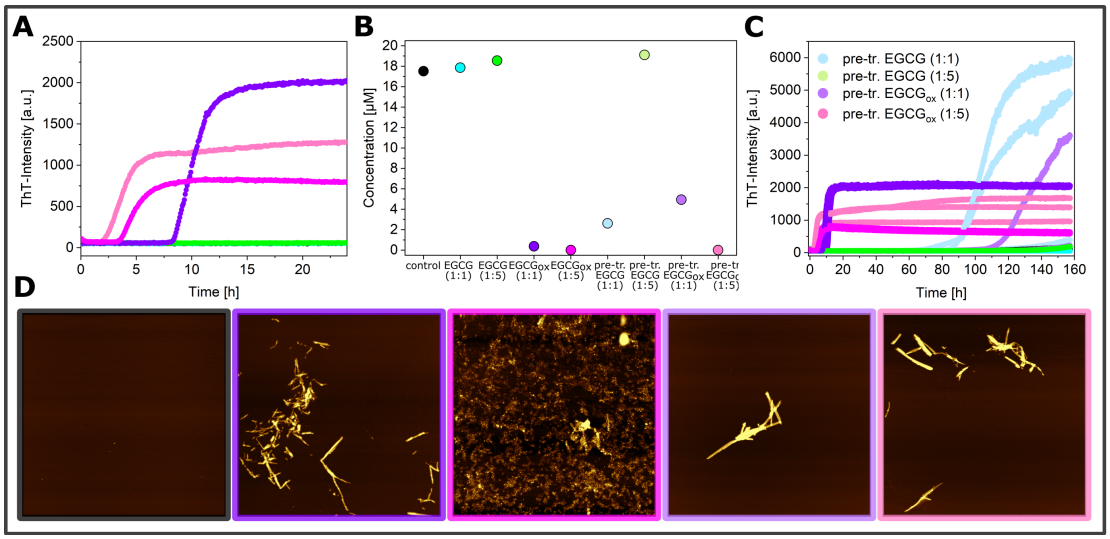

Figure 7. Aggregation kinetics of α-synuclein at pH 4 in a non-binding surface plate under quiescent conditions in absense of glass beads. The fibril formation was monitored in the presence and absence of EGCG or $EGCG_{ox}$, and in wells which were pre-treated with EGCG-solutions (A) and the corresponding concentration measurement by Fluidity One after 160 h (B) with AFM-height-images (D) of the aggregation products of α-synuclein (black frame) in presence of $EGCG_{ox}$ (1:1) (purple frame), (1:5) (magenta frame) and in the pre-treated wells with $EGCG_{ox}$ (1:1) (light purple frame) and (1:5) (light magenta frame) and the overview of the three replicates per condition (C). The image scale is 5 x 5 μM. The colour range represents the height from -3 to 12 nm.

concentration of the 1:1 $EGCG_{ox}$ solution was decreased by 20% and of the 1:5 $EGCG_{ox}$ solution by 28% compared to solutions, which were incubated in an Eppendorf tube for the same time duration. The loss

of ca. 6 μM from the 1:1 EGCG solution, is compatible with the formation of a monolayer of EGCG on the surface of the well, assuming that one molecule can occupy a surface area of approximately 1 nm x 1 nm. It is interesting that at the higher concentration, the EGCG solution is decreases by an approximately proportional amount, which could suggest the formation of supramolecular EGCG structures either in solution or at the surface. Alternatively it could also be explained by a weak binding affinity that leads to saturation of all surface binding sites only at concentrations much higher than the ones used here. Aggregation in the wells treated in this way was indeed found to be accelerated in many cases with respect to the control (Figure 7). In particular, the pre-treatment with $EGCG_{ox}$ was found to be an efficient way to enable the plate to induce α-synuclein aggregation. Most notably, the surface pre-treated with 125 μM $EGCG_{ox}$ is even more efficient (t_{50} of 4.2 h $\pm$ 0.33h) than if the same concentration of 125 μM $EGCG_{ox}$ is present during the aggregation reaction (t_{50} of 4.6 h$\pm$ 0.74 h). In the case of 25 μM $EGCG_{ox}$, pre-treatment was found to be less efficient (t_{50} of more than 120 h) than the presence of the compound (t_{50} of 10.5 h $\pm$ 1.14), suggesting that 25 μM $EGCG_{ox}$ may not be enough to saturate the surface during pre-treatment. This conclusion is in agreement with the one drawn from the EGCG depletion experiments described above. These experiments were performed under quiescent conditions, explaining why some reactions displayed a slower kinetics compared to the equivalent solution conditions in Figure 3 B (control and EGCG 1:1 and 1:5). After the aggregation experiment, we centrifuged the samples and quantified the average size and concentration of the soluble protein by MDS. The samples which did not display an increase in the ThT-fluorescence had indeed remained mostly soluble, whereas the samples with $EGCG_{ox}$ aggregated nearly completely. The intensity I_{max} of the samples in pre-treated wells is higher than the corresponding ones with the same concentrations of EGCG in solution, even though the samples in the wells pre-treated with 25 μM EGCG and $EGCG_{ox}$ contained still a small amount of soluble protein. We could confirm the presence of fibrils of α-synuclein in the pre-treated wells by AFM. The sample with $EGCG_{ox}$ (1:5) present, which corresponds to the time resolved AFM sample in Figure 6 showed mostly amorphous material this time, even though we had seen fibril formation (Figures 3 and 6) with almost identical kinetic traces. This variability in imaging but not in kinetic traces illustrates the fact that AFM imaging is not always representative of the distribution of species in the solution. In addition, the chemical nature of any structure is difficult to ascertain by AFM. The amorphous material in Figure 6 could be protein but also could correspond to the EGCG content of the solution.

Seeded experiments in the presence of EGCG and $EGCG_{ox}$

In all the experiments described above, nucleation and growth of α-synuclein amyloid fibrils proceeds simultaneously, in some cases (pH $<$ 6) in combination with secondary nucleation. A common strategy in the mechanistic analysis of protein aggregation is to perform seeded experiments which can strongly accelerate the overall aggregation time course and which, at high enough seed concentration, allows to study the process of fibril elongation in isolation (Buell et al., 2014; Buell, 2019). Experiments at weaker seeding can be useful if the contribution of secondary processes, such as fibril fragmentation or surface-catalysed secondary nucleation is to be studied (Buell et al., 2014). In the case of α-synuclein, seeded experiments are often performed under quiescent conditions in a non-binding surface plate, in order to minimize the *de novo* formation of fibrils. In order to investigate the effects of EGCG and $EGCG_{ox}$ on the elongation process, we added 5% seeds to monomeric α-synuclein with and without a 5-fold excess of EGCG and $EGCG_{ox}$ with respect to the concentration of monomeric α-synuclein at different pH values (Figure 8). We have recently proposed a definition of a measure for the seeding efficiency of a given batch of seed fibrils, based on the analysis of strongly seeded kinetic data (Buell, 2019). A seeding efficiency of 1 seeding unit (s.u.) corresponds to an effective exponential constant of 1 h^{-1} under conditions where the normalised kinetic traces of the seeded experiments can be well-fitted by the function 1-e^{-kt}, with the time t in hours. We have quantified the following seeded experiments within this framework, allowing for a convenient comparison of the effects of EGCG and $EGCG_{ox}$. It has to be kept in mind, however, that in this framework, the effects of the inhibitor are entirely attributed to their action on the seed fibrils, and interactions with the soluble protein are not included. Therefore this framework is most appropriate for the experiments with pre-incubated seeds.

Fresh EGCG does not show an inhibitory influence on the seeding efficiency, but the fluorescence intensities are decreased in a pH-dependent manner compared to the absence of EGCG. At both pH 3 and 6, the seeding efficiency in the presence of EGCG appears even to be somewhat increased with respect to the control. The strongly seeded aggregation kinetics of α-synuclein at pH 7 in the presence EGCG

Preprints (www.preprints.org) | NOT PEER-REVIEWED | Posted: 3 February 2020 doi:10.20944/preprints202002.0018.v1

Peer-reviewed version available at Int. J. Mol. Sci. 2020, 21, 1995; doi:10.3390/ijms21061995

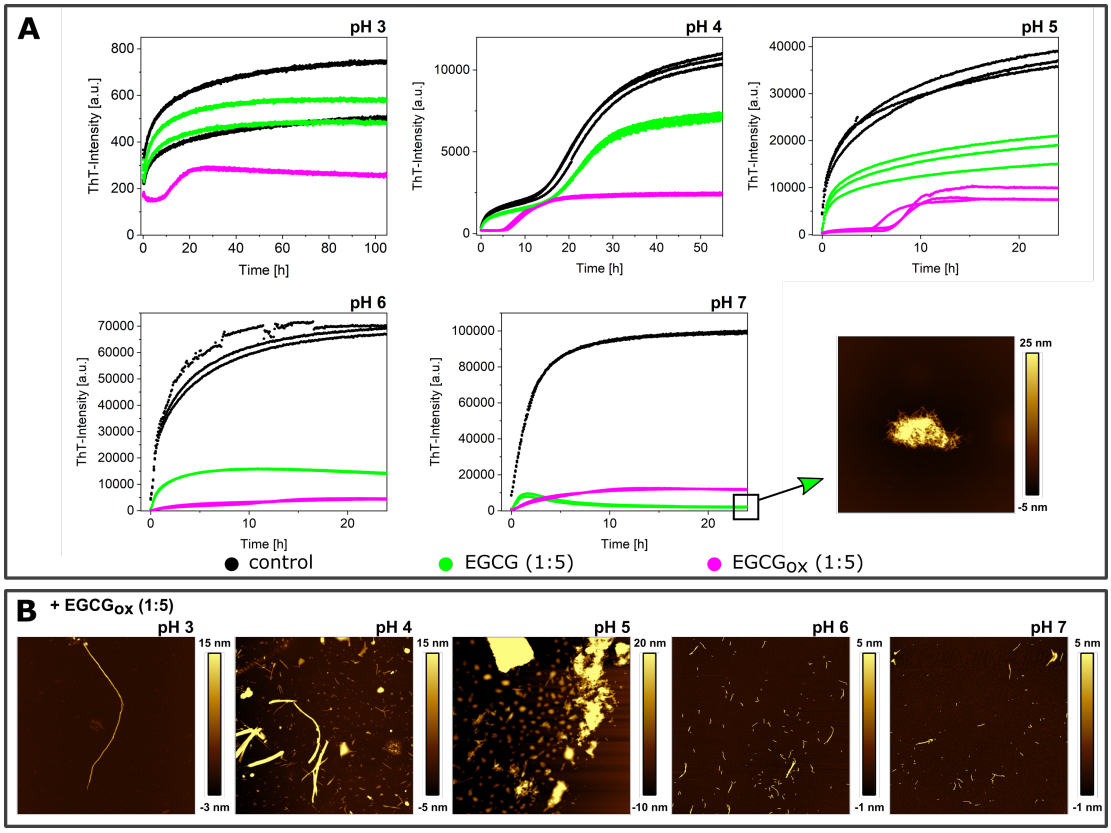

Figure 8. (A) The effects of EGCG and EGCG$_{ox}$ on the aggregation kinetics of α-synuclein, in particular the growth of fibrils, at different pH values (pH 3 to pH 7) in the presence of 5% seeds monitored in a non-binding surface plate under quiescent conditions and a AFM-height-image of the sample at pH 7 in presence of EGCG (1:5) (B) AFM-height-images of α-synuclein in the presence of EGCG$_{ox}$ (1:5) at different pH values after the aggregation experiment. The image scale is 5 x 5 μM.

appear unusual. After a fast increase, the ThT fluorescence intensity decreased strongly. However, by AFM we were able to verify the presence of fibrillar structures. The fibrils were present as big aggregates on the mica substrate (Figure 8 A), which is somewhat unexpected at neutral pH, given that higher order assembly of α-synuclein fibrils is most pronounced at pH values close to the isoelectric point (Buell et al., 2014). The observed decrease in ThT signal could be due to this higher order assembly of the fibrils, or alternatively to the fact that the initial seeded aggregation is faster than the EGCG oxidation, but the latter will ultimately be responsible for a decrease in fluorescence intensity through quenching by the EGCG$_{ox}$. Due to this unusual shape, we did not quantify the seeding efficiency in the presence of EGCG at pH 7. Furthermore, the seeded aggregation at pH 4, both in the presence and absence of EGCG, shows biphasic behaviour, indicative of a contribution of secondary processes, also preventing the application of the simplified framework for the determination of seeding efficiencies. Such behaviour is unexpected at high seed concentrations, but could be explained by higher order assembly which is particularly pronounced close to the isoelectric point (Buell et al., 2014), and which decreases the seeding efficiency. However the similarity of the kinetic traces indicates that also at pH 4, EGCG has no inhibitory effect on the seeding efficiency. The situation is quite different for 1:5 EGCG$_{ox}$, which dramatically reduces the seeding efficiency and leads to sigmoidal aggregation curves at pH 3-5 even at this high seed concentration of 5%. The observed lag times are even longer than in experiments without added seeds in non-binding plates (Figure 9 C). However, these experiments cannot be compared in a straightforward manner, because the non-seeded experiments were performed under shaking conditions and the seeded experiments quiescently. Nevertheless, this result suggests that at the most acidic pH values (3-5), EGCG$_{ox}$ inactivates the pre-formed seeds and the observed ThT intensity increase is due to *de novo* formation of fibrils. AFM-measurement confirmed the presence of fibrils in the samples with EGCG$_{ox}$ under all pH

Preprints (www.preprints.org) | NOT PEER-REVIEWED | Posted: 3 February 2020 doi:10.20944/preprints202002.0018.v1

Peer-reviewed version available at Int. J. Mol. Sci. 2020, 21, 1995; doi:10.3390/ijms21061995

conditions. The fitting of the kinetics which showed the expected shape for strongly seeded experiments (i.e. single exponential function, pH 6-7) reveals a somewhat decreased seeding efficiency with repsect to the control (Figure 9 A).

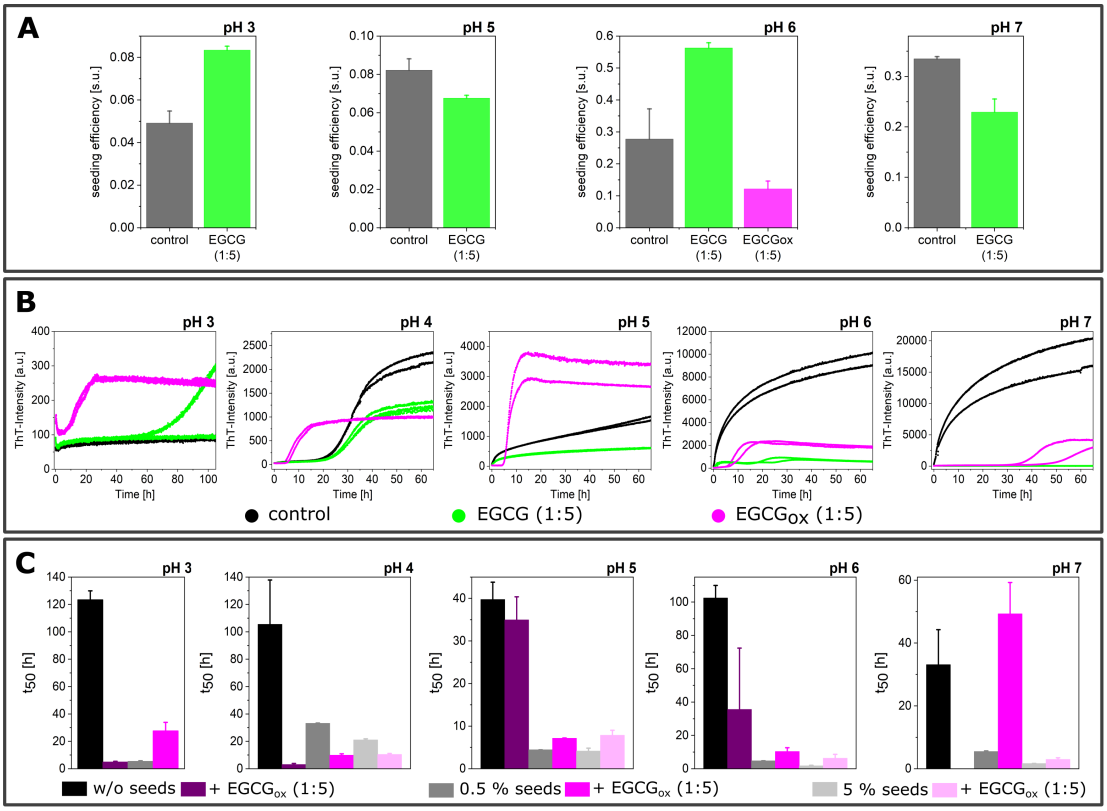

Figure 9. (A) The seeding efficiency, expressed in seeding units (s.u., (Buell, 2019)), determined by fitting the kinetics of the 5% seeding experiments with y=1-e^{-kt} after normalisation between 0 and 1. Only the kinetics which showed the shape expected for a strongly seeded aggregation curve (Buell, 2019) were analysed. (B) The effects of EGCG and EGCG$_{ox}$ on the aggregation kinetics of α-synuclein at different pH values (pH 4 to pH 7) in the presence of 0.5% seeds monitored in a non-binding surface plate under quiescent conditions. (C) The t_{50} of α-synuclein at different pH values (pH 3 to pH 7) in a non-binding surface plate without additional seeds with shaking (filled bar), with 0.5% seeds (striped bar) and 5% seeds (chequered bar) under quiescent conditions and in presence of 1:5 EGCG$_{ox}$ (violet).

When less seeds are added to the experiments (0.5% seeds in monomer equivalents), the aggregation kinetics are considerably slower than at the 10-fold higher seed concentration of the previous experiments (Figure 9B), potentially allowing the impact of EGCG and EGCG$_{ox}$ on secondary processes to be studied. An inhibitory effect of both EGCG and EGCG$_{ox}$ is clearly visible at pH 7. The aggregation starts immediately, without a lag phase, in the control sample, with EGCG$_{ox}$ after over 30 h and in the presence of EGCG, no increase in ThT signal was observed after over 60 h. Compared to the aggregation with 5% seeds, EGCG was therefore found to have a stronger impact on the aggregation kinetics at the decreased seed concentration. EGCG$_{ox}$ also delays the aggregation reaction at pH 5 and pH 6, whereas it has an accelerating effect at pH 4. At the latter pH, the weakly seeded data in the absence of EGCG or EGCG$_{ox}$ has the expected sigmoidal shape indicative of secondary nucleation. The aggregation kinetics in the presence of EGCG$_{ox}$ resembles that in the absence of seeds (Figure 3 and 7), where the EGCG$_{ox}$ induces *de novo* formation of fibrils by changing the properties of the non-binding plate surfaces. Overall, it appears that in these seeded experiments in non-binding plates, several competing effects are at work, all of which are pH-dependent. Fresh EGCG mostly exert its inhibitory effect at pH 7, consistent with the non-seeded experiments. EGCG$_{ox}$, on the other hand, is able to effectively interfere with seeded aggregation at acidic pH values, while at the same time being able to render the non-binding plate

Preprints (www.preprints.org) | NOT PEER-REVIEWED | Posted: 3 February 2020 doi:10.20944/preprints202002.0018.v1

Peer-reviewed version available at Int. J. Mol. Sci. 2020, 21, 1995; doi:10.3390/ijms21061995

conducive to nucleate α-synuclein amyloid fibrils.

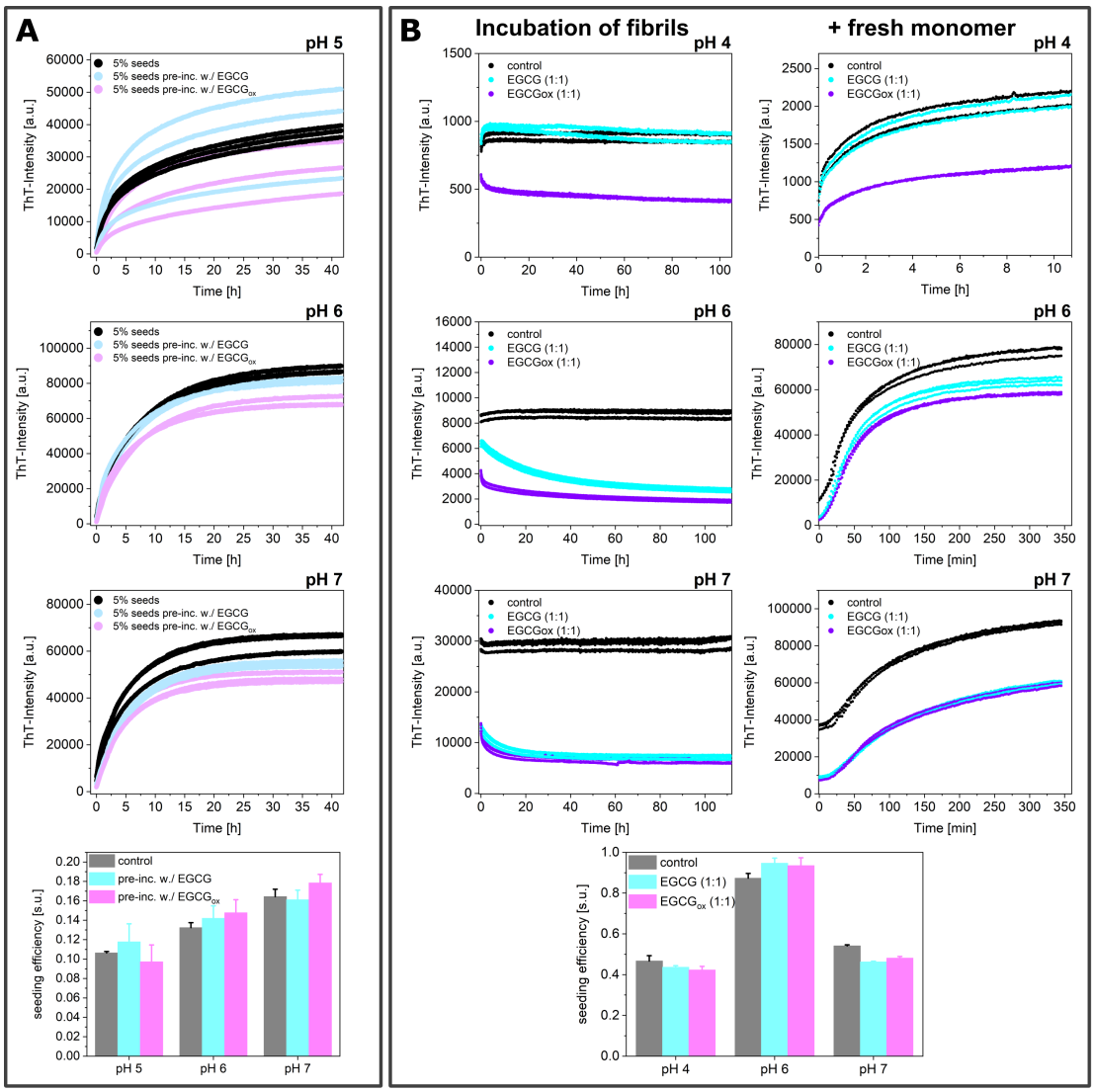

Figure 10. (A) The effects of EGCG and EGCG$_{ox}$ on the seeded aggregation, when the seeds were pre-incubated with stoichiometric amounts of the compound for 2 h at RT before adding them to a 25μM monomer-solution at pH 5, pH 6 and pH 7 to a final concentration of 5% (in monomer equivalents). The samples, where the fibrils were pre-incubated with the compound, contained still 1.25μM EGCG or EGCG$_{ox}$. (B) 10 μM fibrils at pH 4, pH 6 and pH 7 were incubated in presence of 10 μM EGCG or EGCG$_{ox}$ in a non-binding surface plate at 37°C for over 100 h (left) and then 50 μM fresh monomer were added (right).

Experiments in the presence of seeds pre-incubated with EGCG and EGCG$_{ox}$

In order to separate the effects of EGCG on the seeds and on the soluble α-synuclein, we also performed experiments where we incubated seed fibrils for 2 h at room temperature with stoichiometric amounts of EGCG and EGCG$_{ox}$ and added them to a final concentration of 5% (in monomer equivalents) to 25 μM monomeric α-synuclein. This corresponds at the same time to a strong dilution of the EGCG, such that the ratio of soluble α-synuclein to EGCG/EGCG$_{ox}$ is 20:1 during the seeded experiments. If the EGCG either binds with high affinity to the fibrils and/or is able to remodel the fibrils into non-fibrillar structures (Bieschke et al., 2010) then a reduction in seeding efficiency can be expected. However, the observed aggregation kinetics are very similar, particularly when they are normalized to the same final level of fluorescence intensity (Figure 10A). A quantitative analysis shows that the seeding efficiency showed

no significant difference between the samples, suggesting that during the time scale of this experiment, the fibrils have not undergone a significant structural change. In order to investigate whether fibril remodeling into seeding-incompetent species can occur over longer time scales, we incubated 10 μM pre-formed seeds in a non-binding surface plate at 37°C for over 100 h at pH 4, 6 and pH 7 with equimolar concentrations of EGCG or $EGCG_{ox}$ (Figure 10B). The ThT-intensity of the control did not change over time, but the ThT intensity of the fibrillar sample with added EGCG decreased by a factor of 2.4 at pH 6 and 1.8 at pH 7, whereby the decrease at pH 6 was slower. The fluorescence intensity in the presence of oxidised EGCG was reduced by a factor of 2.2 at pH 6 and 2.1 at pH 7. The intensities of the samples with both EGCG and $EGCG_{ox}$ were very similar, the $EGCG_{ox}$ did not lead to a stronger quenching of the fluorescence. Compared to the control, the intensities after over 100 h are lowered by a factor of 3.2 at pH 6 and 4.2 at pH 7 in presence of EGCG and 4.7 in presence of $EGCG_{ox}$. Despite the fact that the significant decrease in ThT fluorescence intensity suggested a change of the seed fibril structure or concentration, and correspondingly a different seeding efficiency, the observed kinetics after addition of 50 μM monomer were virtually identical between all samples. We quantified the seeding efficiencies and found no statistically significant differences induced by the long incubation with EGCG or $EGCG_{ox}$. Therefore an equimolar concentration of EGCG is not able to induce changes in the seeding efficiency of preformed fibrils even after prlonged incubation.

DISCUSSION

The effects of the potential anti-amyloid component EGCG and its auto-oxidised form on the process of amyloid fibril formation of the protein α-synuclein was analysed under distinct environmental conditions. We probed the effect of pH in the range from pH 3 to pH 7, the effect of presence of a glass bead, the influence of the type of plate surface, as well as the presence and absence of seeds, which were either freshly prepared or pre-incubated with EGCG or $EGCG_{ox}$. By examining the change of the maximum ThT-intensity and/or the kinetics of the aggregation (quantified by the t_{50} of the reaction) in presence of the compound, the effects on the *de novo* (i.e. un-seeded) amyloid formation were assessed and a summary is presented in table 1.

The overall picture that emerges from table 1 is that only at pH 7, both I_{max} and t_{50} suggest an inhibitory effect of EGCG under all tested conditions. This is confirmed by microfluidic diffusional sizing experiments, which show that α-synuclein is maintained in its soluble, probably monomeric state by both EGCG and $EGCG_{ox}$. Already at pH 6, the picture becomes more complex and the two parameters I_{max} and t_{50} do not yield a consistent picture: while I_{max} still largely suggests inhibition, t_{50} shows mostly no effect of EGCG but still inhibition for $EGCG_{ox}$. At neutral pH (i.e. pH 7), corresponding to the solution condition most often investigated in previous studies, EGCG is highly unstable. EGCG oxidises rapidly under the investigated buffer conditions within several hours (Sneideris et al., 2019) in a similar time scale as the aggregation process itself in presence of glass beads. A decrease of the pH value to pH 6 leads to a significant increase in the stability of EGCG and accordingly to a less strong inhibitory effect on α-synuclein aggregation. In particular at even lower pH values, where EGCG is highly stable, no significant effects on the *de novo* amyloid fibril formation of α-synuclein are observed. Therefore, mostly the auto-oxidised EGCG is able to inhibit amyloid formation. The fact that I_{max} and t_{50} do not always yield a consistent result strongly suggests that both EGCG and $EGCG_{ox}$ can interfere with ThT fluorescence. It is therefore important to not only rely on ThT intensity alone when assessing the inhibitory effects of EGCG, or indeed any other compound. The inclusion of imaging techniques, such as AFM can help to avoid false positives, but we also show in this work that it can be challenging to obtain representative images of the content of an aggregated protein solution. We therefore employ an additional method in this work, MDS, that allows us to quantify both the concentration and average size of the protein remaining in the supernatant of the completed aggregation reaction after centrifugation. This study reveals the strong influence of the *de novo* aggregation conditions on the mode of action of a given compound. In a non-binding surface plate the presence of EGCG was observed to result in a faster kinetics of aggregation. Unlike the protein, the compound can bind to the non-binding surface and thereby enables α-synuclein monomer to bind to the so-modified surface. This paves the way to the nucleation of amyloid fibrils and starts the amyloid cascade. Consistent with this model, pre-incubation of the wells of a non-binding plate can also lead to efficient induction of aggregation, and a clear concentration dependence of this effect is visible.

To rely solely on the change in ThT intensity as a readout for the extent of inhibition can lead to

Preprints (www.preprints.org) | NOT PEER-REVIEWED | Posted: 3 February 2020 doi:10.20944/preprints202002.0018.v1

Peer-reviewed version available at Int. J. Mol. Sci. 2020, 21, 1995; doi:10.3390/ijms21061995

Table 1. Evaluation of the effects of EGCG and $EGCG_{ox}$ on the *de* novo α-synuclein aggregation process established by comparing experimental values of I_{max} or t_{50} of the control samples (α-synuclein) with the ones determined in the presence of the component using one-way ANOVA (*:$p < 0.05$; **:$p < 0.01$; ***:$p < 0.001$). If the effect is defined as inhibitory without indication of the p-value, the sample showed no aggregation during the term. The abbreviations HBS stands for high-binding surface, NBS for non-binding surface and GB for glass bead.

	Assessed by change in I_{max}				
	Conditions	EGCG (1:1)	EGCG (1:5)	$EGCG_{ox}$ (1:1)	$EGCG_{ox}$ (1:5)
physiologically relevant conditions					
pH 7	HBS + GB	Inhibitory***	Inhibitory***	Inhibitory***	Inhibitory***
	HBS - GB	Inhibitory*	Inhibitory*	Inhibitory*	Inhibitory*
	NBS + GB	Inhibitory***	Inhibitory***	Inhibitory***	Inhibitory***
	NBS - GB	No effect	Inhibitory***	Inhibitory***	Inhibitory***
pH 6	HBS + GB	Inhibitory***	Inhibitory***	Inhibitory***	Inhibitory***
	HBS - GB	Inhibitory*	No effect	Inhibitory*	Inhibitory*
	NBS + GB	No effect	No effect	Inhibitory*	Inhibitory*
	NBS - GB	Enhancing**	No effect	Enhancing***	No effect
pH 5	HBS + GB	No effect	Inhibitory***	Inhibitory***	Inhibitory***
	HBS - GB	No effect	No effect	No effect	Inhibitory**
	NBS + GB	No effect	No effect	No effect	Inhibitory***
	NBS - GB	No effect	No effect	Enhancing***	No effect
pH 4	HBS + GB	No effect	No effect	Inhibitory*	Inhibitory***
	HBS - GB	No effect	Inhibitory**	No effect	Inhibitory***
	NBS + GB	No effect	No effect	No effect	No effect
	NBS - GB	Enhancing**	No effect	Enhancing*	No effect
pH 3	HBS + GB	No effect	No effect	No effect	Inhibitory***
	HBS - GB	No effect	No effect	No effect	Inhibitory**
	NBS + GB	No effect	Inhibitory*	Inhibitory***	Inhibitory***
	NBS - GB	No effect	No effect	No effect	No effect

	Assessed by change in t_{50}				
	Conditions	EGCG (1:1)	EGCG (1:5)	$EGCG_{ox}$ (1:1)	$EGCG_{ox}$ (1:5)
physiologically relevant conditions					
pH 7	HBS + GB	Inhibitory	Inhibitory	Inhibitory	Inhibitory
	HBS - GB	Inhibitory**	Inhibitory	Inhibitory	Inhibitory
	NBS + GB	Inhibitory	Inhibitory	Inhibitory**	No effect
	NBS - GB	No effect	Inhibitory	No effect	Inhibitory
pH 6	HBS + GB	No effect	No effect	Inhibitory*	Inhibitory
	HBS - GB	Inhibitory**	Enhancing*	Inhibitory***	Inhibitory
	NBS + GB	No effect	No effect	No effect	Inhibitory
	NBS - GB	No effect	No effect	No effect	No effect
pH 5	HBS + GB	No effect	No effect	No effect	Inhibitory**
	HBS - GB	No effect	No effect	No effect	No effect
	NBS + GB	Enhancing**	Enhancing**	Enhancing**	No effect
	NBS - GB	No effect	Inhibitory***	Enhancing*	No effect
pH 4	HBS + GB	No effect	No effect	No effect	Inhibitory***
	HBS - GB	No effect	No effect	No effect	No effect
	NBS + GB	No effect	Enhancing**	Enhancing***	No effect
	NBS - GB	Enhancing**	Enhancing**	Enhancing***	Enhancing***
pH 3	HBS + GB	No effect	No effect	Inhibitory*	No effect
	HBS - GB	No effect	No effect	No effect	Enhancing**
	NBS + GB	Enhancing**	Enhancing***	Enhancing***	Enhancing*
	NBS - GB	No effect	No effect	Enhancing**	Enhancing**

erroneous interpretation of a given compound as an inhibitor (e.g. EGCG seemed to inhibit the aggregation at pH 6 in a high-binding plate with glass beads, but the t_{50} and the soluble protein at the end of the measurement showed no effect on the amyloid formation). In particular the oxidised EGCG strongly quenches ThT fluorescence, rather than inhibiting amyloid fibril growth. The compound either interferes with ThT-fluorescence (Buell et al., 2010) or binds to amyloid fibrils, preventing the binding of ThT (Palhano et al., 2013; Sneideris et al., 2019).

A *de novo* experiment involves different microscopic steps. At neutral pH conditions the process is dominated by primary nucleation, growth and fragmentation. Secondary nucleation on the surface of preformed α-synuclein fibrils becomes more important, when the pH is decreased towards the isoelectric point. By performing seeded experiments the investigation of the process of fibril elongation in isolation is feasible. In strongly seeded (5% seeds in monomer equivalents), mostly $EGCG_{ox}$ exerts an effect on the

seeding efficiency, and this inhibitory effect appears most pronounced at acidic pH values. At the lowest pH values, *de novo* aggregation, aided by the coating of the wells by EGCG, become efficient enough to lead to rapid aggregation despite the lack of seeding. More weakly seeded experiments (0.5% seeds in monomer equivalents) are more susceptible to inhibition, probably because the relative concentration ratio of inhibitor to seed is higher. These seeded experiments provide clear evidence for an interaction between α-synuclein fibrils and both EGCG and $EGCG_{ox}$ under most pH conditions. This is consistent with a previous study that has reported an affinity of EGCG for α-synuclein fibrils in the low μM range at neutral pH (Wolff et al., 2016). Indeed, in this previous work, it was noted that the affinity of EGCG to α-synuclein fibrils appeared to become more tight over the course of minutes to hours. This corresponds to the time scale of EGCG oxidation under these conditions and is consistent with our finding here that $EGCG_{ox}$ has a stronger inhibitory effect at equivalent concentrations. We also performed an experiment to probe whether $EGCG_{ox}$ interacts with fibrils at more acidic pH than what had been shown in the previous study. When 25 μM α-synuclein fibrils are incubated with a stoichiometric quantity of $EGCG_{ox}$, approximately two thirds of the compound can be centrifuged down with the fibrils. This result confirms that α-synuclein fibrils interact with $EGCG_{ox}$ also at acidic pH with a stoichiometry not very different from 1:1.

Since we detected an inhibitory effect of $EGCG_{ox}$ in seeded experiments, particularly in the experiments at low seed concentrations, we tested whether incubating the seeds with EGCG or $EGCG_{ox}$ before the experiment was able to influence their seeding efficiency. In experiments where the seeds were incubated for 1 h and then added at a final concentration of 5% in monomer equivalents at pH 5-7, the aggregation kinetics and the efficiency of the seeds did not reveal any differences between pre-incubated seeds and those that had not been in contact with EGCG or $EGCG_{ox}$. We then tested whether the seeds were altered by a substantially longer incubation ($> 100\ h$) at 37°C, followed by addition of fresh monomer. Also here we found no influence on the seeding efficiency, but the ThT fluorescence intensity was strongly decreased by the compounds. In these pre-incubation experiments, the concentrations of EGCG/$EGCG_{ox}$ is sub-stoichiometric during the actual elongation reaction. Taken together, our seeded experiments show therefore that EGCG and/or its oxidation products can only act on the seeding efficiency if present at high enough concentrations and that the interactions between the seeds and the compound are not able to permanently alter the seeding efficiency.

This finding agrees with a previous observation for κ-casein fibrils, which interact with high affinity with EGCG, but showed no indication of modification the structure or of redirection of the aggregation pathway (Hudson et al., 2009). However, various studies have reported the EGCG-induced remodelling of diverse amyloid fibrils and a formation of soluble amorphous aggregates at neutral pH (Bieschke et al., 2010; Palhano et al., 2013; Shoval et al., 2008; Ehrnhoefer et al., 2008; Zhao et al., 2017; Zhu et al., 2016; Chandrashekaran et al., 2011; He et al., 2009; Daniels et al., 2019). Our seeding data did not suggest a seeding efficiency change or dissociation of the pre-formed α-synuclein fibrils; EGCG interacts with the fibril surface and therefore changes the interaction with ThT, as well as being able to interfere with the seeding if present at sufficiently high concentrations. However, an equimolar concentration is not sufficient to change the structure of preformed fibrils in such a way to render them less efficient as seeds.

All together, our results paint a much more complex picture of the inhibitory effects of EGCG on the amyloid fibril formation by α-synuclein than what the available literature suggests. We summarize our findings in Figure 11. First of all, EGCG itself seems to be very ineffective as inhibitor, whereas its oxidation products are much more efficient (Sneideris et al., 2019). This finding explains why in general EGCG is a rather inefficient inhibitor in *de novo* experiments under pH conditions where EGCG is stable, i.e. mildly acidic pH. Furthermore, EGCG can interact with non-binding surfaces of plates and transform them into efficient surfaces for the heterogeneous primary nucleation of α-synuclein amyloid fibrils. Finally, $EGCG_{ox}$ is able to effectively interfere with seeded aggregation if present at a high enough ratio with respect to the seeds. However, upon dilution and subsequent unbinding, the fibrils recover their seeding efficiency. Our seeded experiments were carried out under quiescent conditons, where fibril fragmentation is negligible and no new ends are therefore generated, explaining the efficient inhibition. Under conditions of vigorous mechanical shaking, such as the ones we have employed in our *de novo* experiments, the constant generation of new ends through primary nucleation and fragmentation (Buell et al., 2014) renders the inhibitory effect of $EGCG_{ox}$ much weaker. Our study represents the most detailed investigation of the inhibitory effects of EGCG on α-synuclein amyloid fibril formation. From our study emerges a complete picture of the EGCG effect on α-synuclein aggregation. This data suggest that an

Preprints (www.preprints.org) | NOT PEER-REVIEWED | Posted: 3 February 2020 doi:10.20944/preprints202002.0018.v1

Peer-reviewed version available at Int. J. Mol. Sci. 2020, 21, 1995; doi:10.3390/ijms21061995

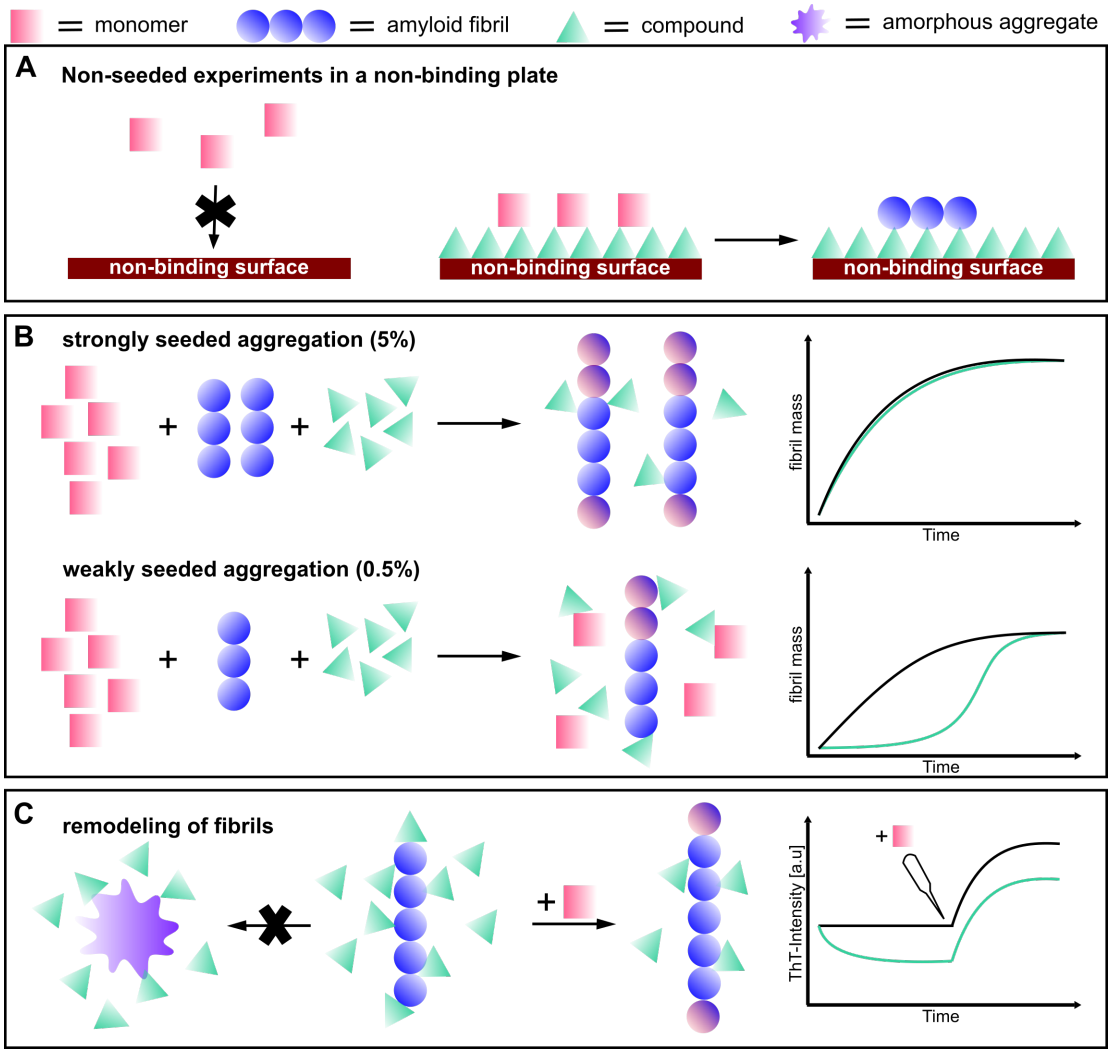

Figure 11. Schematic depiction of monitored effects of the anti-amyloid compound EGCG on the α-synuclein fibril formation. (A) shows that α-synuclein can not bind to the non-binding surface of the plate, while the compound EGCG can bind to the surface and facilitate the formation of amyloid fibrils. (B) EGCG displayed almost no effect on a strongly seeded aggregation (5% seeds), whereas a weakly seeded aggregation (0.5% seeds) could be retarded through interactions with the monomer. (C) The compound seems to interact with amyloid fibrils, but was not able to remodel the fibril into amorphous aggregates. When fresh monomer was added, the fibrils could elongate like the control.

extensive characterisation of potential amyloid fibril inhibitors is required in order to be able to conclude whether a given molecule is a useful inhibitor.

CONCLUSIONS

In conclusion, we have shown that EGCG only inhibits the amyloid fibril formation by α-synuclein under very specific conditions, and that this compound can even act as an enhancer of amyloid fibril formation through facilitating heterogeneous primary nucleation. The oxidation products of EGCG are significantly more efficient inhibitory agents than the unmodified EGCG, but at the same time it is also more efficient in inducing primary nucleation. This leads to a complex interplay of the inhibitory and enhancing effects of EGCG and $EGCG_{ox}$, the net effects of which depend on the pH of the solution, the presence or absence of seeds, as well as the type of reaction vessel and the general conditions of the aggregation reaction. Importantly, we also establish that EGCG is not able to remodel α-synuclein into seed-incompetent structures. Taken together our results highlight the complexity of even such a supposedly well-established

amyloid inhibitor as EGCG and establish a detailed experimental strategy to evaluate the true potential of a compound to interfere with amyloid fibril formation.

ACKNOWLEDGMENTS

AKB and AP thank the Parkinson's and Movement Disorder Foundation for funding. RSH thanks the Manchot Foundation for financial support. AKB thanks the Novo Nordisk Foundation for funding through a Novo Nordisk Foundation Professorship.

REFERENCES

Aarsland, D., Londos, E., and Ballard, C. (2009). Parkinson's disease dementia and dementia with lewy bodies: different aspects of one entity. *International psychogeriatrics*, 21(2):216–219.

Agerschou, E. D., Flagmeier, P., Saridaki, T., Galvagnion, C., Komnig, D., Nagpal, A., Gasterich, N., Heid, L., Prasad, V., Shaykhalishahi, H., Willbold, D., Dobson, C. M., Voigt, A., Falkenburger, B., Hoyer, W., and Buell, A. K. (2019). An engineered monomer binding-protein for α-synuclein efficiently inhibits the proliferation of amyloid fibrils. *eLife*, 8:e46112.

Arosio, P., Muüller, T., Rajah, L., Yates, E. V., Aprile, F. A., Zhang, Y., Cohen, S. I., White, D. A., Herling, T. W., De Genst, E. J., et al. (2015). Microfluidic diffusion analysis of the sizes and interactions of proteins under native solution conditions. *ACS nano*, 10(1):333–341.

Baba, M., Nakajo, S., Tu, P.-H., Tomita, T., Nakaya, K., Lee, V., Trojanowski, J. Q., and Iwatsubo, T. (1998). Aggregation of alpha-synuclein in lewy bodies of sporadic parkinson's disease and dementia with lewy bodies. *The American journal of pathology*, 152(4):879.

Bertoncini, C. W., Jung, Y.-S., Fernandez, C. O., Hoyer, W., Griesinger, C., Jovin, T. M., and Zweckstetter, M. (2005). Release of long-range tertiary interactions potentiates aggregation of natively unstructured alpha-synuclein. *Proceedings of the National Academy of Sciences of the United States of America*, 102:1430–1435.

Bieschke, J., Russ, J., Friedrich, R. P., Ehrnhoefer, D. E., Wobst, H., Neugebauer, K., and Wanker, E. E. (2010). EGCG remodels mature α-synuclein and amyloid-β fibrils and reduces cellular toxicity. *Proceedings of the National Academy of Sciences*, 107(17):7710–7715.

Bourdenx, M., Bezard, E., and Dehay, B. (2014). Lysosomes and α-synuclein form a dangerous duet leading to neuronal cell death. *Frontiers in Neuroanatomy*, 8:83.

Braak, H. and Braak, E. (1991). Neuropathological stageing of alzheimer-related changes. *Acta neuropathologica*, 82(4):239–259.

Bucciantini, M., Giannoni, E., Chiti, F., Baroni, F., Formigli, L., Zurdo, J., Taddei, N., Ramponi, G., Dobson, C. M., and Stefani, M. (2002). Inherent toxicity of aggregates implies a common mechanism for protein misfolding diseases. *nature*, 416(6880):507.

Buell, A. K. (2019). The growth of amyloid fibrils: rates and mechanisms. *Biochemical Journal*, 476(19):2677–2703.

Buell, A. K., Dobson, C. M., Knowles, T. P., and Welland, M. E. (2010). Interactions between amyloidophilic dyes and their relevance to studies of amyloid inhibitors. *Biophysical journal*, 99(10):3492–3497.

Buell, A. K., Galvagnion, C., Gaspar, R., Sparr, E., Vendruscolo, M., Knowles, T. P. J., Linse, S., and Dobson, C. M. (2014). Solution conditions determine the relative importance of nucleation and growth processes in α-synuclein aggregation. *Proc Natl Acad Sci U S A*, 111(21):7671–7676.

Campioni, S., Carret, G., Jordens, S., Nicoud, L., Mezzenga, R., and Riek, R. (2014). The presence of an air-water interface affects formation and elongation of alpha-synuclein fibrils. *J Am Chem Soc*.

Chandrashekaran, I. R., Adda, C. G., MacRaild, C. A., Anders, R. F., and Norton, R. S. (2011). Egcg disaggregates amyloid-like fibrils formed by plasmodium falciparum merozoite surface protein 2. *Archives of biochemistry and biophysics*, 513(2):153–157.

Chiti, F. and Dobson, C. M. (2017). Protein misfolding, amyloid formation, and human disease: A summary of progress over the last decade. *Annual Review of Biochemistry*, 86(1):27–68.

Cohen, S. I. A., Linse, S., Luheshi, L. M., Hellstrand, E., White, D. A., Rajah, L., Otzen, D. E., Vendruscolo, M., Dobson, C. M., and Knowles, T. P. J. (2013). Proliferation of amyloid-β42 aggregates occurs through a secondary nucleation mechanism. *Proc Natl Acad Sci U S A*, 110(24):9758–9763.

Daniels, M. J., Nourse, J. B., Kim, H., Sainati, V., Schiavina, M., Murrali, M. G., Pan, B., Ferrie, J. J.,

Haney, C. M., Moons, R., et al. (2019). Cyclized ndga modifies dynamic α-synuclein monomers preventing aggregation and toxicity. *Scientific reports*, 9(1):2937.

Ehrnhoefer, D. E., Bieschke, J., Boeddrich, A., Herbst, M., Masino, L., Lurz, R., Engemann, S., Pastore, A., and Wanker, E. E. (2008). Egcg redirects amyloidogenic polypeptides into unstructured, off-pathway oligomers. *Nature structural & molecular biology*, 15(6):558.

Ehrnhoefer, D. E., Duennwald, M., Markovic, P., Wacker, J. L., Engemann, S., Roark, M., Legleiter, J., Marsh, J. L., Thompson, L. M., Lindquist, S., Muchowski, P. J., and Wanker, E. E. (2006). Green tea (-)-epigallocatechin-gallate modulates early events in huntingtin misfolding and reduces toxicity in Huntington's disease models. *Human Molecular Genetics*, 15(18):2743–2751.

Fusco, G., Simone, A. D., Gopinath, T., Vostrikov, V., Vendruscolo, M., Dobson, C. M., and Veglia, G. (2014). Direct observation of the three regions in α-synuclein that determine its membrane-bound behaviour. *Nat Commun*, 5:3827.

Galvagnion, C., Buell, A. K., Meisl, G., Michaels, T. C. T., Vendruscolo, M., Knowles, T. P. J., and Dobson, C. M. (2015). Lipid vesicles trigger α-synuclein aggregation by stimulating primary nucleation. *Nat Chem Biol*, 11(3):229–234.

Gang, H., Galvagnion, C., Meisl, G., Müller, T., Pfammatter, M., Buell, A. K., Levin, A., Dobson, C. M., Mu, B., and Knowles, T. P. J. (2018). Microfluidic diffusion platform for characterizing the sizes of lipid vesicles and the thermodynamics of protein-lipid interactions. *Analytical chemistry*, 90:3284–3290.

Gaspar, R., Meisl, G., Buell, A. K., Young, L., Kaminski, C. F., Knowles, T. P., Sparr, E., and Linse, S. (2017). Secondary nucleation of monomers on fibril surface dominates α-synuclein aggregation and provides autocatalytic amyloid amplification. *Quart Rev Biophys*, 50.

Grey, M., Linse, S., Nilsson, H., Brundin, P., and Sparr, E. (2011). Membrane interaction of α-synuclein in different aggregation states. *J Parkinsons Dis*, 1(4):359–371.

Guerrero-Ferreira, R., Taylor, N. M., Mona, D., Ringler, P., Lauer, M. E., Riek, R., Britschgi, M., and Stahlberg, H. (2018). Cryo-em structure of alpha-synuclein fibrils. *eLife*, 7:e36402.

He, J., Xing, Y.-F., Huang, B., Zhang, Y.-Z., and Zeng, C.-M. (2009). Tea catechins induce the conversion of preformed lysozyme amyloid fibrils to amorphous aggregates. *Journal of agricultural and food chemistry*, 57(23):11391–11396.

Hudson, S. A., Ecroyd, H., Dehle, F. C., Musgrave, I. F., and Carver, J. A. (2009). (-)-epigallocatechin-3-gallate (egcg) maintains κ-casein in its pre-fibrillar state without redirecting its aggregation pathway. *Journal of molecular biology*, 392(3):689–700.

Iljina, M., Hong, L., Horrocks, M. H., Ludtmann, M. H., Choi, M. L., Hughes, C. D., Ruggeri, F. S., Guilliams, T., Buell, A. K., Lee, J.-E., Gandhi, S., Lee, S. F., Bryant, C. E., Vendruscolo, M., Knowles, T. P. J., Dobson, C. M., De Genst, E., and Klenerman, D. (2017). Nanobodies raised against monomeric α-synuclein inhibit fibril formation and destabilize toxic oligomeric species. *BMC biology*, 15:57.

Knowles, T. P. J., Vendruscolo, M., and Dobson, C. M. (2014). The amyloid state and its association with protein misfolding diseases. *Nature reviews. Molecular cell biology*, 15(6):384–96.

Lee, Y.-H., Lin, Y., Cox, S. J., Kinoshita, M., Sahoo, B. R., Ivanova, M., and Ramamoorthy, A. (2019). Zinc boosts EGCG's hIAPP amyloid Inhibition both in solution and membrane. *Biochimica et Biophysica Acta (BBA) - Proteins and Proteomics*, 1867(5):529 – 536.

Liu, Y., Liu, Y., Wang, S., Dong, S., Chang, P., and Jiang, Z. (2015). Structural characteristics of (-)-epigallocatechin-3-gallate inhibiting amyloid Aβ42 aggregation and remodeling amyloid fibers. *RSC Advances*, 5(77):62402–62413.

Luk, K. C., Kehm, V., Carroll, J., Zhang, B., O'Brien, P., Trojanowski, J. Q., and Lee, V. M.-Y. (2012). Pathological α-synuclein transmission initiates parkinson-like neurodegeneration in nontransgenic mice. *Science*, 338(6109):949–953.

Mak, S. K., McCormack, A. L., Manning-Bog, A. B., Cuervo, A. M., and Monte, D. A. D. (2010). Lysosomal degradation of alpha-synuclein in vivo. *Journal of Biological Chemistry*, 285:13621–13629.

McClendon, S., Rospigliosi, C. C., and Eliezer, D. (2009). Charge neutralization and collapse of the c-terminal tail of alpha-synuclein at low ph. *Protein Science*, 18(7):1531–1540.

Meisl, G., Kirkegaard, J. B., Arosio, P., Michaels, T. C., Vendruscolo, M., Dobson, C. M., Linse, S., and Knowles, T. P. (2016). Molecular mechanisms of protein aggregation from global fitting of kinetic models. *Nature protocols*, 11(2):252.

Murray, A. N., Palhano, F. L., Bieschke, J., and Kelly, J. W. (2013). Surface adsorption considerations when working with amyloid fibrils in multiwell plates and eppendorf tubes. *Protein Science*,

668 22(11):1531–1541.
669 na Díaz, S. P., Pujols, J., Conde-Giménez, M., Carija, A., Dalfo, E., García, J., Navarro, S., Pinheiro, F.,
670 Santos, J., Salvatella, X., Sancho, J., and Ventura, S. (2019). Zpd-2, a small compound that inhibits
671 α-synuclein amyloid aggregation and its seeded polymerization. *Front Mol Neurosc*.
672 Palhano, F. L., Lee, J., Grimster, N. P., and Kelly, J. W. (2013). Toward the molecular mechanism (s) by
673 which egcg treatment remodels mature amyloid fibrils. *Journal of the American Chemical Society*,
674 135(20):7503–7510.
675 Pandey, K. B. and Rizvi, S. I. (2009). Plant polyphenols as dietary antioxidants in human health and
676 disease. *Oxidative medicine and cellular longevity*, 2(5):270–278.
677 Peduzzo, A., Linse, S., and Buell, A. (2019). The Properties of α-Synuclein Secondary Nuclei are
678 Dominated by the Solution Conditions Rather than the Seed Fibril Strain.
679 Perni, M., Galvagnion, C., Maltsev, A., Meisl, G., Müller, M. B. D., Challa, P. K., Kirkegaard, J. B.,
680 Flagmeier, P., Cohen, S. I. A., Cascella, R., Chen, S. W., Limbocker, R., Sormanni, P., Heller, G. T.,
681 Aprile, F. A., Cremades, N., Cecchi, C., Chiti, F., Nollen, E. A. A., Knowles, T. P. J., Vendruscolo, M.,
682 Bax, A., Zasloff, M., and Dobson, C. M. (2017). A natural product inhibits the initiation of α-synuclein
683 aggregation and suppresses its toxicity. *Proc Nat Acad Sc*, 114(6):E1009–E1017.
684 Pillay, C. S., Elliott, E., and Dennison, C. (2002). Endolysosomal proteolysis and its regulation. *Biochem-*
685 *ical Journal*, 363(3):417–429.
686 Qing, H., McGeer, P. L., Zhang, Y., Yang, Q., Dai, R., Zhang, R., Guo, J., Wong, W., Xu, Y., and Quan, Z.
687 (2016). Epigallocatechin gallate (EGCG) inhibits alpha-synuclein aggregation: A potential agent for
688 Parkinson's disease. *Neurochemical Research*, 41(10):2788–2796.
689 Rambold, A. S., Miesbauer, M., Olschewski, D., Seidel, R., Riemer, C., Smale, L., Brumm, L., Levy, M.,
690 Gazit, E., Oesterhelt, D., et al. (2008). Green tea extracts interfere with the stress-protective activity of
691 prpc and the formation of prpsc. *Journal of neurochemistry*, 107(1):218–229.
692 Roberts, B. E., Duennwald, M. L., Wang, H., Chung, C., Lopreiato, N. P., Sweeny, E. A., Knight, M. N.,
693 and Shorter, J. (2009). A synergistic small-molecule combination directly eradicates diverse prion
694 strain structures. *Nature Chemical Biology*, 5(12):936–946.
695 Roy, S. and Bhat, R. (2019). Suppression, disaggregation, and modulation of γ-Synuclein fibrillation
696 pathway by green tea polyphenol EGCG. *Protein Science*, 28(2):382–402.
697 Shoval, H., Weiner, L., Gazit, E., Levy, M., Pinchuk, I., and Lichtenberg, D. (2008). Polyphenol-induced
698 dissociation of various amyloid fibrils results in a methionine-independent formation of ros. *Biochimica*
699 *et Biophysica Acta (BBA)-Proteins and Proteomics*, 1784(11):1570–1577.
700 Sneideris, T., Sakalauskas, A., Sternke-Hoffmann, R., Peduzzo, A., Ziaunys, M., Buell, A. K., and
701 Smirnovas, V. (2019). The environment is a key factor in determining the anti-amyloid efficacy of egcg.
702 *Biomolecules*, 9(12):855.
703 Spillantini, M. G., Crowther, R. A., Jakes, R., Hasegawa, M., and Goedert, M. (1998). α-synuclein
704 in filamentous inclusions of lewy bodies from parkinson's disease and dementia with lewy bodies.
705 *Proceedings of the National Academy of Sciences*, 95(11):6469–6473.
706 Srinivasan, E. and Rajasekaran, R. (2017). Probing the inhibitory activity of epigallocatechin-gallate
707 on toxic aggregates of mutant (L84F) SOD1 protein through geometry based sampling and steered
708 molecular dynamics. *Journal of Molecular Graphics and Modelling*, 74:288–295.
709 Teng, Y., Zhao, J., Ding, L., Ding, Y., and Zhou, P. (2019). Complex of egcg with cu (ii) suppresses
710 amyloid aggregation and cu (ii)-induced cytotoxicity of α-synuclein. *Molecules*, 24(16):2940.
711 Theillet, F.-X., Binolfi, A., Bekei, B., Martorana, A., Rose, H. M., Stuiver, M., Verzini, S., Lorenz, D.,
712 van Rossum, M., Goldfarb, D., and Selenko, P. (2016). Structural disorder of monomeric α-synuclein
713 persists in mammalian cells. *Nature*, 530:45–50.
714 Tóth, G., Gardai, S. J., Zago, W., Bertoncini, C. W., Cremades, N., Roy, S. L., Tambe, M. A., Rochet,
715 J.-C., Galvagnion, C., Skibinski, G., Finkbeiner, S., Bova, M., Regnstrom, K., Chiou, S.-S., Johnston,
716 J., Callaway, K., Anderson, J. P., Jobling, M. F., Buell, A. K., Yednock, T. A., Knowles, T. P. J.,
717 Vendruscolo, M., Christodoulou, J., Dobson, C. M., Schenk, D., and McConlogue, L. (2014). Targeting
718 the intrinsically disordered structural ensemble of α-synuclein by small molecules as a potential
719 therapeutic strategy for parkinson's disease. *PLoS One*, 9(2):e87133.
720 Uversky, V. N., Li, J., and Fink, A. L. (2001). Evidence for a partially folded intermediate in α-synuclein
721 fibril formation. *Journal of Biological Chemistry*, 276(14):10737–10744.
722 van der Wateren, I. M., Knowles, T., Buell, A., Dobson, C. M., and Galvagnion, C. (2018). C-terminal

truncation of α-synuclein promotes amyloid fibril amplification at physiological ph. *Chemical Science*.

Wagner, J., Ryazanov, S., Leonov, A., Levin, J., Shi, S., Schmidt, F., Prix, C., Pan-Montojo, F., Bertsch, U., Mitteregger-Kretzschmar, G., Geissen, M., Eiden, M., Leidel, F., Hirschberger, T., Deeg, A. A., Krauth, J. J., Zinth, W., Tavan, P., Pilger, J., Zweckstetter, M., Frank, T., Bähr, M., Weishaupt, J. H., Uhr, M., Urlaub, H., Teichmann, U., Samwer, M., Bötzel, K., Groschup, M., Kretzschmar, H., Griesinger, C., and Giese, A. (2013). Anle138b: a novel oligomer modulator for disease-modifying therapy of neurodegenerative diseases such as prion and parkinson's disease. *Acta Neuropathol*, 125:795–813.

Wei, Y., Chen, P., Ling, T., Wang, Y., Dong, R., Zhang, C., Zhang, L., Han, M., Wang, D., Wan, X., et al. (2016). Certain (-)-epigallocatechin-3-gallate (egcg) auto-oxidation products (eaops) retain the cytotoxic activities of egcg. *Food chemistry*, 204:218–226.

Wobst, H. J., Sharma, A., Diamond, M. I., Wanker, E. E., and Bieschke, J. (2015). The green tea polyphenol (-)-epigallocatechin gallate prevents the aggregation of tau protein into toxic oligomers at substoichiometric ratios. *FEBS Letters*, 589(1):77–83.

Wolff, M., Mittag, J. J., Herling, T. W., De Genst, E., Dobson, C. M., Knowles, T. P., Braun, D., and Buell, A. K. (2016). Quantitative thermophoretic study of disease-related protein aggregates. *Scientific reports*, 6(1):1–10.

Wood, S. J., Wypych, J., Steavenson, S., Louis, J.-C., Citron, M., and Biere, A. L. (1999). α-synuclein fibrillogenesis is nucleation-dependent implications for the pathogenesis of parkinson's disease. *Journal of Biological Chemistry*, 274(28):19509–19512.

Xu, Z. X., Ma, G. L., Zhang, Q., Chen, C. H., He, Y. M., Xu, L. H., Zhou, G. R., Li, Z. H., Yang, H. J., and Zhou, P. (2017). Inhibitory mechanism of epigallocatechin gallate on fibrillation and aggregation of amidated human islet amyloid polypeptide. *ChemPhysChem*, 18(12):1611–1619.

Yates, E. V., Müller, T., Rajah, L., De Genst, E. J., Arosio, P., Linse, S., Vendruscolo, M., Dobson, C. M., and Knowles, T. P. J. (2015). Latent analysis of unmodified biomolecules and their complexes in solution with attomole detection sensitivity. *Nature chemistry*, 7:802–809.

Zhao, J., Liang, Q., Sun, Q., Chen, C., Xu, L., Ding, Y., and Zhou, P. (2017). (-)-Epigallocatechin-3-gallate (EGCG) inhibits fibrillation, disaggregates amyloid fibrils of α-synuclein, and protects PC12 cells against α-synuclein-induced toxicity. *RSC Advances*, 7(52):32508–32517.

Zhu, W., Peng, J.-M., Ge, Z.-Z., and Li, C.-M. (2016). A-type dimeric epigallocatechin-3-gallate (egcg) is a more potent inhibitor against the formation of insulin amyloid fibril than egcg monomer. *Biochimie*, 125:204–212.